University of Tartu
Faculty of Science and Technology
Institute of Ecology and Earth Sciences
Department of Geography

Master Thesis in Geoinformatics for Urbanized Society (30 ECTS)

Detecting the Greening of Mu Us Sandy Land by using Remote Sensing

Peng WANG

Supervisors: Prof. Tõnu Oja

Tartu 2021

Lühikokkuvõte

Selles uurimustöös analüüsitakse erinevatel ruumilistel ja ajalistel skaaladel kvalitatiivselt ja kvantitatiivselt Maowusu kõrbe taimedega kaetuse dünaamikat perioodil 1986–2020. Analüüs põhineb Landsati kogu 1. astme andmetel, kliimaandmetel ja NASADEM-i andmetel. Samal ajal uuriti ka NDVI, RSEI ja veel kolme ökoloogilise näitaja (NDSI, Wet, LST) võimalikku suhet. Maowusu kõrbe ökoloogilise muutumise seireks ja hindamiseks kasutati spetsiaalselt ökoloogilise indeksi põhist kaugseiret (RSEI). Nimetatud indeksi all on kokku võetud neli olulist ökoloogilist näitajat, mida keskkonna hindamisel sageli kasutatakse. Need on rohelus, kuivus, märgus ja kuumus. Neid nelja näitajat esindavad vastavalt neli RS-i näitajat, mis on NDVI, NDSI, Wet ja LST.
Tulemused näitavad järgmist.
(1) 1986. aastal oli uuritud ala kõrbestumise etapis ning selle taimedega kaetus oli peamiselt vähene ja kõrbestunud ala moodustas kokku 87% uuritud alast. 2020. aastaks on kõrbestumise ohje abil saavutatud märkimisväärseid tulemusi. Vähene taimedega kaetus on suuresti asendunud keskmise ja suure taimedega kaetusega ning kõrbestunud ala on umbes 30% võrra vähenenud.
(2) Mitmekesise reljeefiga alad pakuvad taimestikule parema kasvukeskkonna ja vähene taimestikuga kaetus muutub seal kiiresti rohkeks. Tasasel maastikul on kasvutingimused halvemad ja taimestikuga kaetuse määr muutub väga aeglaselt. NDVI väärtused on teatud määral seotud ka maapinna kallakuga.
(3) Kõikehõlmava ökokeskkonna hindamise indeks on koos taimedega kaetuse suurenemisega kasvanud. Taimedega kaetuse suurenemine on osaliselt tingitud ka Weti suurenemisest ja LST ja NDBSI vähenemisest.

Võtmesõnad: Maowusu kõrb, NDVI, kõrbestumine, RSEI, GEE, kaugseire
CERCS-i kood: T181 kaugseire

Abstract

In this paper, dynamics of vegetation cover on different spatial and temporal scales in Mu Us Sand Land were qualitatively and quantitatively analyzed for the period from 1986 to 2020, based on Landsat Collection 1 Tier 1, climate data, and NASADEM; meanwhile, conducting studies to tease out the potential relationship among NDVI, RSEI and other three ecological indicators (NDSI, Wet, LST). A remote sensing based ecological index (RSEI) was applied specially for monitoring and assessing ecological changes of Mu Us Sand Land, the index combined four important ecological indicators which are frequently used in evaluating ecology. These are greenness, dryness, wetness, and heat. The four indicators were represented respectively by four RS indices, which are the NDVI, NDSI, Wet, and LST.

The results show that:

(1) In 1986, the study area was in the desertification stage, and its vegetation coverage was mainly low, accounting for 87% of the total study area. By 2020, desertification control has achieved remarkable results. The low vegetation coverage is mainly replaced by medium and high vegetation coverage and has been reduced to about 30%.

(2) Topographic relief areas provide vegetation better growing habitats, and the vegetation coverage rate changes rapidly from low to high. While in flat terrain, the growing habitats are worse, and the vegetation coverage rate here changes very slowly. Furthermore, NDVI values are related to the slope to a certain degree.

(3) the comprehensive eco-environment appraisal index has gone up, with the improvement of vegetation coverage; Moreover, the increase of vegetation coverage partly results in the increase in Wet and the decrease in LST and NDBSI.

Keywords: Mu Us Sandy Land, NDVI, Desertification, RSEI, GEE, Remote Sensing
CERCS code: T181 Remote Sensing

Contents

Introduction

From an ecological and socio-economic perspective, land degradation is considered as one of the significant global issues today to be threatening the well-being of no less than 3.2 billion people (especially rural communities, smallholder farmers, and the very poor), costing over 10 percent of the annual global gross product in terms relating to biodiversity loss and ecosystem services, even driving the sixth mass extinction of species as a main factor (Scholes, IPBES 2018). Kumar et al.(2014) hold the view that climate change is recognized as a major factor responsible for land degradation, but we realized mutual influences and relations between climate change and land degradation; between 2000 and 2009, land degradation was responsible for annual global emission of 3.6-4.4 billion tonnes of CO_2 (IPBES 2018) as a driver of climate change through the emission of greenhouse gases (GHGs) (Olsson, 2019), which aggravates CO_2-induced climate change by way of the release of CO_2 from cleared and dead vegetation and by reducing the carbon sequestration potential of degraded land (Arrazia et al., 2014). By 2050, global cereal production is projected to fall by an average of 10 percent, and in some regions could reach 50 percent, primarily due to land degradation and climate change (Montanarella, IPBES 2018). The instability of society will be fueled without timely action to avoid, reduce and reverse land degradation; Scholes (IPBES 2018) predicts that 4 billion people will be living in drylands in 2050, while 50 to 700 million people may be forced to migrate. There are many different definitions of land degradation in the literature, with different emphases on biodiversity, ecosystem functions, and ecosystem services (Olsson, 2019). The United Nations Convention to Combat Desertification (UNCCD) defines land degradation as a ‘reduction or loss, in arid, semi-arid, and dry sub-humid areas, of the biological or economic productivity and complexity of rain-fed cropland, irrigated cropland, or range, pasture, forest, and woodlands resulting from land uses or from a process or combination of processes, including processes arising from human activities and habitation patterns, such as: (i) soil erosion caused by wind and/or water; (ii) deterioration of the physical, chemical, and biological or economic properties of soil; and (iii) long-term loss of natural vegetation (WMO, 2005).’ The land degradation mentioned in this paper refers mainly to the loss of life-supporting land resources through soil erosion, desertification, salinization, etc. The term ‘Desertification’ here is seen as a form of land degradation by which fertile land becomes desert (WHO, 2020).

The phenomenon of desertification has been around for a long time, but the scientific understanding of its causes and consequences is very recent. 'Desertification' was first popularised by French botanist André Aubréville in 1948, which used to describe how tropical forest regions in Africa were being transformed into 'desert-like regions'

(Cherlet et al., 2018). Nevertheless, the term 'desertification' was first used by Lavauden to describe the low productivity of Tunisian pastures in 1927 (Becerril-Piña et al., 2020). In the early 1960s, over-farming contributed to wide-scale land degradation in the blackland prairies in the central part of the former Soviet Union, repeating the history about 'Black Sunday (storm)' that occurred on April 14, 1935, in northern Texas, which also promoted research on soil wind erosion and land management in the former Soviet Union. The Sahel region in West Africa is well known for its persistently unsolved environmental problems of drought and desertification (Agnew et al., 1999). From the late 1960s to the early 1980s, drought-induced famine in the Sahel region killed 100,000 people, while most of the 50 million people had been affected to varying degrees (UNEP, 2002). At the end of the 1970s, desertification became one of the most important scientific issues worldwide (Plit et al., 1995). Since then, the United Nations passed the General Assembly Resolution of 3337 on ’Plan of Action to Combat Desertification’ in 1975 (Zheng, 2009), and adopted this plan in 1977, which is regarded as the beginning of the milestones of United Nations Convention to Combat Desertification (UNCCD) (Chasek et al., 2016). The 1977 Nairobi meeting of the United Nations Conference on Desertification (UNCOD) informed by 1st world map of desertification made by the Food and Agriculture Organization (FAO), the United Nations Environment Programme (UNEP) and the United Nations Educational, Scientific and Cultural Organization (UNESCO) (Lu, 2014.; Jia, 2018). Furthermore, a definition of desertification was proposed as ‘… the diminution or destruction of the biological potential of the land, (which) can lead ultimately to desert-like conditions’ (UNCD, 1977.; Wang, 2013). Common to numerous definitions of desertification until today means that desertification is perceived as an adverse environmental process, which essentially matches the description regarding desertification in the definition as ‘land degradation in arid, semi-arid, and dry sub-humid areas resulting from various factors, including climatic variations and human activities’ stated by the UNEP (1994). In addition, several scholars with different opinions exist, including one that has been cited many times so far, which is the definition used by Dregne (1986) himself as ‘desertification is the impoverishment of terrestrial ecosystems under the impact of man. It is the process of deterioration in these ecosystems that can be measured by reduced productivity of desirable plants, undesirable alterations in the biomass and the diversity of the micro and macro fauna and flora, accelerated soil deterioration, and increased hazards for human occupancy.’

Although desertification is a phenomenon that exists in almost all regions, it has a high concentration in Africa and Asia (GEF&GM 2006). An estimated 40% of people in Africa and Asia live in areas under constant threat of desertification (Stather, 2006.; Ambalam, 2014). China is severely affected by desertification, with 17.93 percent of

its territory covered in the desert (Li et al., 2019), which has the highest number of deserts in Asia (Misachi, 2020.; Ren et al., 2015). Desertification is a dominant ecological problem in northwest China, which increasingly limits the development of the local economy (Cao, 2011). Intending to control desertification, the government of China promulgated 'Law of the People's Republic of China on Prevention and Control of Desertification' on August 31, 2001. Moreover, implemented a series of large-scale mitigation programs, including the Three-North Shelterbelt Programme, to establish 35 million ha of shelterbelt forests between 1978 and 2050 (SFA PRC, 2018). A focus of these projects is on the vegetative cover increase through the prohibition of open-grazing, the planting of trees and grasses, and the construction of shelterbelt to the protection of farmland against blowing sand (Feng et al., 2015). Since 1993, the country has been conducting national desertification and sandification monitoring at 5-year intervals, and has now done so five times (Tu et al., 2016). The latest monitoring results indicated that as of 2014, desertified land and sandy land in China were 2,161,600 square kilometers and 1,721,200 square kilometers, respectively. By comparison with 2009, the desertified land area has been reduced by a net 12,120 square kilometers over the past five years, with a reduction of 2,424 square kilometers per year on average, while the sandy land area has been reduced by a net 9,902 square kilometers, with a reduction of 1,980 square kilometers per year on average (SFA PRC, 2015). With investments in desertification control totaling approximately US$6.49 billion over the period 2013 to 2018, the cumulative area of sandy to be controlled in China is over 10 million hectares. (NFGA, 2018). As expressed by the Shaanxi Provincial Forestry Bureau, Yulin, located within the Mu Us Sandy Land, reversed desertification at an annual rate of 1.62%, resulting in a 93.24% rate of sandy land structural consolidation in Yulin by April 2020, while forest cover percentage increased from the initial 0.9% to 34.8%, and sandy land area reduced from 2.4 million hectares to 1.35 million hectares (Li, 2021). This study selected the Mu Us Sandy Land, where Yulin is located, as the study object, by interpreting long time-series of remote sensing images to examine both the changes in vegetation and the eco-environmental changes in the study area.

Concerning the numerous characteristics of the Mu Us Sandy Land’s ecosystem, such as its importance and fragility, extensive research has been carried out to examine the ecological and environmental problems faced by the Mu Us Sandy Land from various aspects. Its analysis was first conducted in terms of climate and environment, with patterns of past and future climatic and environmental changes in the Mu Us Sandy Land revealed and predicted, respectively. Secondly, numerous scholars have conducted comprehensive studies on the vegetation of the Mu Us Sandy Land from multiple different perspectives to contribute to a deeper study regarding the ecosystem of the Mu Us Sandy Land (Zhang, 2006).

While the results derived from traditional fieldwork-based ecological data provide a fragmentary assessment of ecosystem functions, in contrast, the application of remote sensing techniques may be efficient in estimating the functions of an entire ecosystem simultaneously. Remote sensing of vegetation is capable of measuring ecosystem function at multiple spatial scales that are most comparable to the extent of human-induced environmental changes (Rocchini et al., 2004). Measuring NDVI values, in particular in combination with land-use data, is increasingly vital for distinguishing between natural variability in ecosystem function and changes caused by human activities. NDVI is also somewhat variable in high-agricultural and urban areas, with a high correlation to the degree of vegetation cover (Oindo et al., 2002), which can be used to detect a land cover change and as an indicator of landscape heterogeneity and biodiversity, thereby identifying priority conservation areas and predicting suitable species for that habitat (Hao, 2019). In this paper, NDVI was used as an indicator to monitor vegetation coverage changes in the study area, while RSEI was used as an ecological index to assess the ecological condition of the desert, with the aim of acquiring a macroscopic understanding of the vegetation coverage and ecological environment within the study area over the last four decades. There are three primary objectives and relevant questions as following, that were proposed in the study:

- Monitoring and evaluating vegetation status in Mu Us Sandy Land for long time series,

Q: How did vegetation index and coverage change in Mu Us Sandy Land from 1986 to 2020

- Finding out the effect of topographic gradient on vegetation coverage in Mu Us Sandy land

Q: Is vegetation coverage change related to topographic gradient?
How did vegetation coverage change as affected by different degrees of topographic gradient?

- Detecting and evaluating ecological changes in Mu Us Sandy Land for long time series.

Q: How did RSEI-based ecological index change in study area in 1990, 2005, 2019?

Is there existing a strong correlation between NDVI, RSEI, and other three indicators (LST, NDBSI, Wet) in Study Area? How did they change while the increase of NDVI values?

The following section of this paper consists of four parts. The first part focuses on applying remote sensing to monitor vegetation and an overview of the study area in theory. The second part describes the data and methods used in this study. The last two parts contain the analysis of the outcomes and conclusions, respectively.

1. Theoretical Overview

1.1 Applications of Remote Sensing Technology in Desertification Research

Nowadays, the amount and availability of multitemporal images is experiencing an immediate increase as space exploration technologies continue to evolve. The application solutions in any fields can be solved by various remote sensing data types such as optical passive sensor images, multi-to hyper-spectral data, multi-to hyper-temporal data, active SAR images, etc. (Bovolo et al., 2018).

But decades ago, in a historical context in which still single data or even no remote sensing data was available for solving problems, an incipient combination of aerial information occurred to solve geographical problems since the 1970s. In 1975, Lamprey, based on a vegetation map, a climatic map, and aerial field investigations, affirmed that the southern limit of the Sahara was advancing at the rate of 5.5 km per year (Mainguet, 2012). Following the United Nations Conference on Desertification in 1977, Berry et al. (1977) proposed a four-tier system of indicators for monitoring desertification at the global, regional, national, and local scales. However, this system revealed a severe problem in that human activities were not sufficiently taken into account. Although Reining (1978) subsequently developed a monitoring indicator system consisting of numerous indicators within the physical, biological and social domains, this indicator system is excessively theoretical and lacking in practical application in consideration of the interconnectedness between natural and human factors. Otterman (1977) and Walker et al.(1981), both of whom noted the influence of anthropogenic factors in their studies, used the Landsat multispectral scanner (MSS) imagery to conclude that the brightness of albedo is strongly related to the quality of the land, with greater albedo values leading to more significant degradation of land quality.

Researches based on remote sensing techniques have been carried out comparatively frequently since the 1990s. Tucker et al. (1991, 1994) evaluated the distribution and transition of the Sahara Desert with NDVI derived from NOAA/AVHRR satellite data and demonstrated a strong correlation between the desert and precipitation changes. Moreover, time-series NOAA/AVHRR data have been widely used in desertification research. Li et al. (2002) used the modified soil-adjusted vegetation index (MSAVI) during vegetation growing seasons derived from time-series NOAA/AVHRR data to monitor the dynamic processes of sandy desertification occurring in the western sandy lands of the Northeast China Plain between 1990 and 1997. Liu et al. (2004) assessed the multi-year dynamics of desertification in arid and semi-arid zones of the deserts in Western China for the period 1982 to 2000 using NOAA/AVHRR time series data. Meanwhile, some scholars were using Landsat satellite data to monitor and evaluate

desertification status in the Mawusu Desert and Northwest China. Wu et al. (1997) conducted dynamic monitoring regarding the desertification inside the Mu Us Sandy Land by processing and analyzing TM data for 1987 and 1993. According to the results, the total area of desertified land in the study area decreased by 1936 km^2 over the seven years, with an overall stable reversal; substantially all of the reversal resulted from the reduction in fixed and semi-fixed mobile dunes. Guo et al. (2008) collected Landsat 7 ETM+ in 2000 and Landsat 5 TM in 2005, integrated with aeolian desertification land data of 1977 and 1986, which were used to monitor and analyze the spatial distribution and dynamic changes of desertified land in Mu Us Sandy Land and its surrounding areas in different periods. They indicated that during 1977 – 2005, the area of aeolian desertification land decreases continuously in all counties or banners of the study area. Furthermore, there was a study carried out by Yan et al. (2013) to retrieve the desertification process in Mu Us Sandy Land over the past 40 years using Landsat images from 1977 to 2010 as remote sensing data and method coupled with decision tree classification and ISODATA unsupervised classification. Zhou (2019) conducted a comprehensive study on desertification's spatial and temporal evolution caused by sanding, salinization, and water erosion in the study area in 1975, 2000, and 2017 based on the multi-scale classification of desert types in mainland China. The spatial and temporal evolution patterns of desertification in different periods were obtained by comparing the percentage changes of an area in different desertification areas.

A significant increase in the number of studies combining the digital evaluation model (DEM) to analyze the relationship between desertification and topographic relief followed around 2010 due to improvements in the quality of DEM data (Hu et al., 2010; Liu et al., 2015; Hu et al., 2020). The morphological characteristics of sand dunes are an important element in the study of wind and sand modeled landscapes. DEM are widely used in sand dune morphology and dynamics studies with their superior capability of 3D terrain representation (Wang, 2020). According to Duan's (2013) analysis on the relationship between aeolian desertified land and terrain factor, which showed the area and severity of aeolian desertified land gradually reduced with the increasing elevation, yet, the distribution of aeolian desertified land had no significant changes with the slope variation.

1.2 Evolution in Vegetation Monitoring with Remote Sensing-based Technology

Numerous ecosystems are being affected by climate change on a global scale, notably rising temperatures caused impacts and costs of 1.5 degrees Celsius of global warming are far greater than expected (IPCC, 2018). Considered as an essential component of terrestrial ecosystems, the response of vegetation to climate change is particularly significant. Examples include the increased photosynthetic activity of vegetation at

high northern latitudes as a consequence of climate warming (Myneni et al., 1997), and vegetation in the Alps spreading over a higher altitude range than before (Grabherr et al., 1994). Vegetation change is considered an indicator of global change to a certain extent due to the high sensitivity of vegetation to climate change (Ma et al., 2006), which has therefore continued to receive long-term attention from researchers (Tucker et al., 1986; Stenseth et al., 2002; Zeng et al., 2009). There is variability in the effects of different climatic conditions on vegetation. Kawabata et al. (2001) analyzed interannual trends in annual and seasonal vegetation activities from 1982 to 1990 on a global scale to show that the increase in temperature at mid to high latitudes in the northern hemisphere has led to a marked increase in vegetation activities. In contrast, in the arid and semi-arid regions of the southern hemisphere, diminishing annual precipitation has led to a gradual weakening of plant photosynthesis and, ultimately, a reduction in vegetation activities. The significant relationship between vegetation and precipitation generally occurs in arid and semi-arid regions with distinct climatic differences during the wet and dry seasons, especially in arid and semi-arid ecosystems where both the onset and duration of vegetation growth are generally controlled by precipitation (Spano et al., 1999). Ichii et al. (2002) analyzed the global vegetation-climate relationship on an interannual scale and found that the positive correlation between vegetation and precipitation occurred in Central Asia, the southern Sahara, South Africa, Australia, and southern South America, where the influence of precipitation on vegetation was dominant, even though temperature also influenced vegetation to some extent in these regions. Philippon et al. (2005) found a conspicuous seasonal dependence in the relationship between NDVI and precipitation in Sahel and Guinea, with the correlation between them occurring mainly during the rainy season, which is also usually the growing season for vegetation. Xin et al. (2007) concluded that NDVI in the Loess Plateau region of China is sensitive to precipitation and considered that precipitation plays a decisive role in the region's spatial distribution. In addition, vegetation changes in arid-semi-arid transition areas show an undoubtedly positive response to precipitation (Dekker et al., 2007).

Some studies have mainly been interested in research objectives concerning monitoring vegetation cover changes in Mu Us Sandy Land in the last few years. Liu et al. (2009) analyzed the dynamic variation of vegetation coverage based on NDVI in 1990 and 2007, and then found low vegetation coverage (NDVI < 0.3) was the main body which area declined from 33176.7369 km^2 in 1990 to 30671.6454 km^2 in 2007, annual change rate was – 0.048%. Moderate vegetation coverage (NDVI 0.3 – 0.6) and high vegetation coverage (NDVI > 0.6) changed from 1313.5023 km^2 in 1990 to 3818.5938 km^2 in 2007, annual changing rate were 3.91% and 3.48% respectively. Huang et al. (2014) followed this up with a study of the changes in vegetation cover in the Mu Us Sandy

Land during the decade 2000 to 2010 based on MODIS-NDVI, and they concluded a substantial increase in grassland area in the study area, in particular between 2005 and 2010. A trend of gradual increase in vegetation cover in the Mu Us Sandy Land during this decade was observed, with a highly significant increase in the north-western and south-eastern parts of the study area. Yan et al. (2013) found the vegetation growth trends in annual maximum value that mainly fluctuates slightly in Mu Us Sandy Land from 2000 to 2011; the worst status of vegetation growth is in 2001, and the best is in 2010.

1.3 Study Area

1.3.1 Overview of the Study Area

The Mu Us Sandy Land is also known as the Maowusu Desert or Mu Us desert. We are more inclined to call sandy land it as its type of desertification is sandy desertification, which is land degradation characterized by wind erosion mainly resulted from the excessive human activities in arid, semiarid and part of sub-humid regions in northern China (Wang, 2014; Zhang, 2020). It covers an area of about 42,200 km^2, lying at 37.45°N-39.37°N, 107.67°E-110.5°E, mainly in the southern part of Ordos City in Inner Mongolia, the northern part of Yulin City in Shaanxi Province and the northeastern part of Yanchi County in Ningxia Hui Autonomous Region, which as a transitional zone forms part of Ordos Plateau and includes part of the Loess Plateau alluvial plain with a concave floor (Han, 2019). (Figure 1.1)

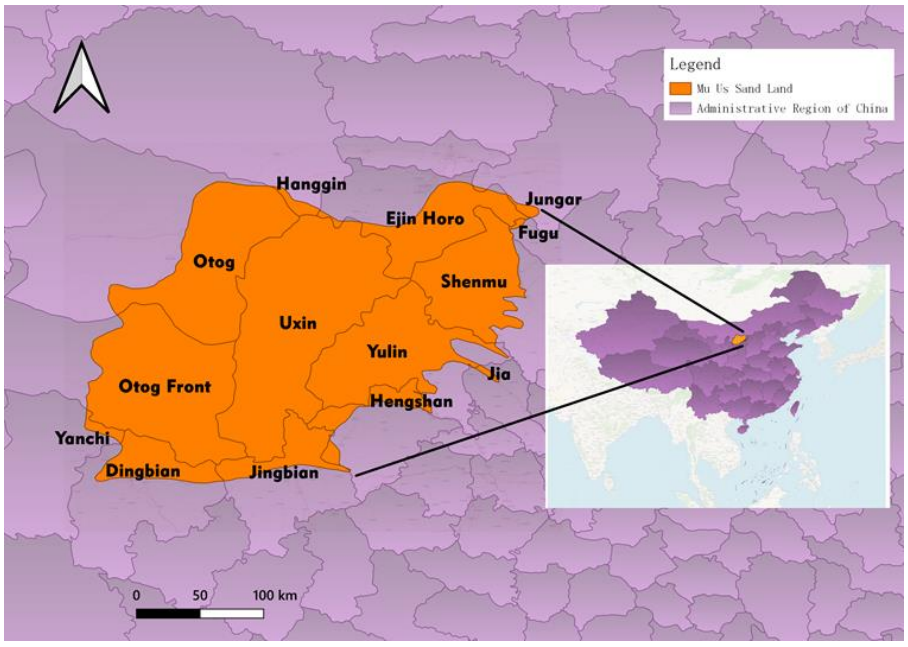

Figure 1.1 Location of the Study Area - Mu Us Sandy Land

1.3.2 Vegetation Condition

The central and eastern parts of the Mu Us Sandy Land are in the dry grassland subzone, the northwestern edge is in the desert grassland subzone towards the desert transition, and the southeastern edge trends towards forest grassland in terms of climatic zones. The vegetation in the study area is mainly covered by semi-fixed and fixed dunes, sand land, dried mudflats and agricultural land. In the plant cover stipa glareosa, stipa gobica, artemisia frigida were predominantly found on agricultural land, and caragana korshinskii kom, hedysarum mongolicum turcz, artemisia sphaerocephala, salix psammophila, salix psammophila and artemisia ordosica were mainly in shrubs for sandy soils (Han, 2019).

1.3.3 Precipitation Condition

Although annual precipitation in the Mu Us Sandy Land fluctuates repeatedly, the overall trend is increasing. 567.175 mm was the highest value in 36 years in 2016, falling to 303.711 mm in 2020 (Figure 1.2). As shown in Figure 1.3, precipitation in these three years is generally concentrated in the eastern and northeastern parts of the study area, with the lowest precipitation in the west. The highest precipitation in 2020 was 411.13 mm and the lowest was 231.49 mm. on the while, the precipitation condition in the Mu Us Sandy Land is quite satisfactory.

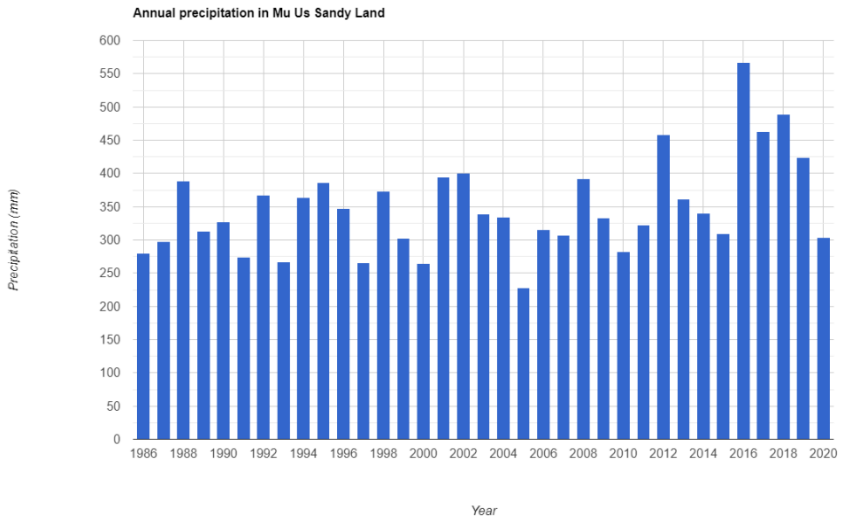

Figure 1.2 The Trends of Annual Precipitation in Mu Us Sandy Land

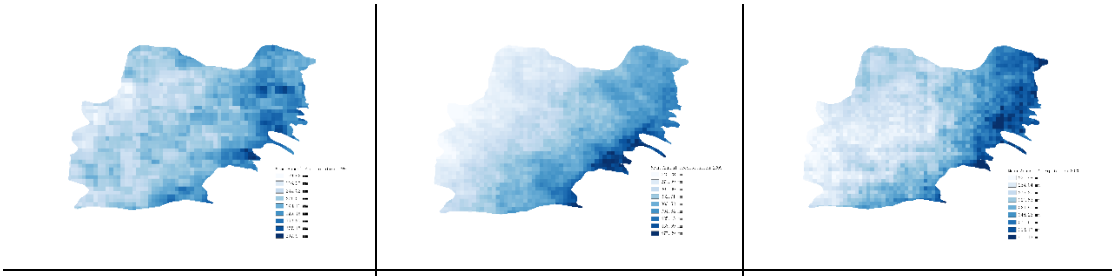

Figure 1.3 Annual Precipitation in 1986, 2009, 2020

1.3.4 Topographic Condition

As part of the Ordos Plateau, the elevation ranges from 980m to 1,320m (as low as 906m in some south-eastern valleys, and reaching between 1,434m to 1,610m in the north-western area) (Figure 1.4). This is the only one of the twelve sandy regions of China that lies in the transition zone between the typical grassland and desert climate.

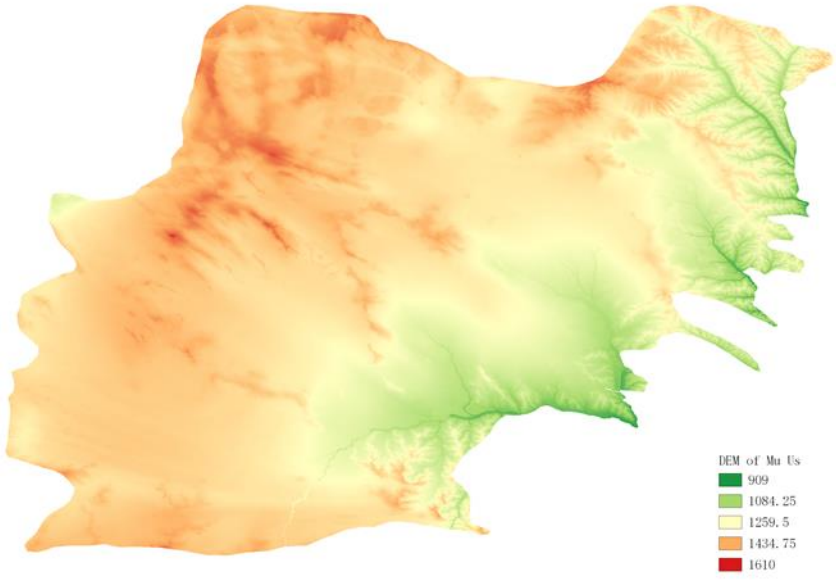

Figure 1.4 DEM of Mu Us Sandy Land

2. Data and Methods

2.1 Data

2.1.1 Used Landsat Collections for Vegetation Coverage

The aim of this paper to monitor vegetation changes in the study area over the last forty years, considering the Landsat series of satellites could provide sufficient free image data for this study, which is the main reason why other satellite data were not applied in this study, such as MODIS, which was launched until 2000.

In 1967, NASA proposed the Earth Resources Technology Satellite program, which began a theoretical feasibility study for two Earth observation satellites were individually known as ERTS-A and ERTS-B (Wells et al.1976). as shown in Figure 2.1, Landsat 1 was launched on July 23, 1972; at that time, the satellite was known as the Earth Resources Technology Satellite (ERTS) used for remote sensing of land resources on Earth. Later in the 1970s and 1980s, successively more Landsat satellites were launched. Landsat 6 was failed in launch, Landsat 7 was launched in 1999, followed by Landsat 8, which was launched on 11 February 2013.

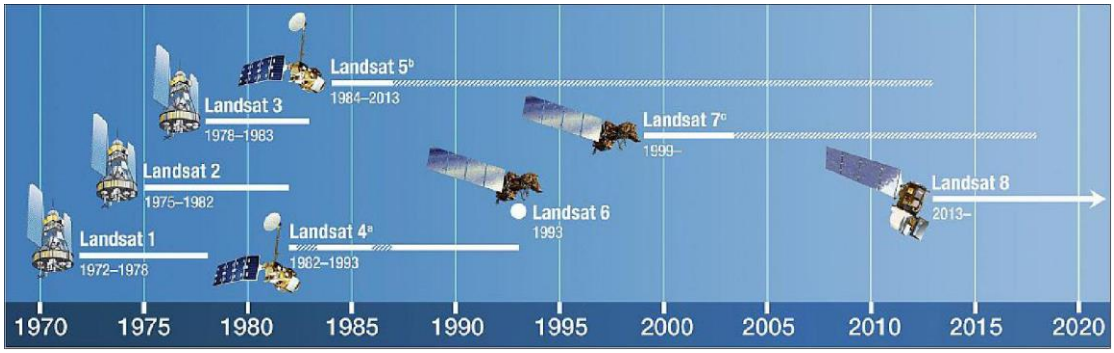

Figure 2.1 SLI (Sustainable Land Imaging) architecture, past and ongoing missions (image credit: NASA)

The data was used to extract the maximum value of NDVI every two years, derived from Landsat 5 collection 1 Tier1, Landsat 7 collection 1 Tier1, and Landsat 8 collection 1 Tier1 in GEE online database. We filtered the Landsat 7 SLC-off data with bad pixel or blackline before exporting the result. After that, the total number of remote sensing images we used in this study is shown in Table 2.1. Data covering the study area from 1986 to 2020, with a total of 6185 scenes (see Table 3.5), which includes 2787 scenes of Landsat 5(TM) data, 2390 scenes of Landsat7(ETM) data, and 1008 scenes of Landsat8(OLI)data. Figure 2.2 shows the time series of Landsat images corresponding to each of the data I used in this study. The quality of the data for the years 1986, 1990, and 1999 was not favorable.

Table 2.1 Used Landsat Data Amount

Periods \ Sensors	TM data	ETM data	OLI data	Subtotal
1986-1987	136	-	-	136
1988-1989	207	-	-	207
1990-1991	207	-	-	207
1992-1993	249	-	-	249
1994-1995	216	-	-	216
1996-1997	209	-	-	209
1998-1999	197	14	-	211
2000-2001	248	201	-	449
2002-2003	213	210	-	423
2004-2005	242	234	-	476
2006-2007	215	201	-	416
2008-2009	221	220	-	441
2010-2011	227	176	-	403
2012-2013	-	211	78	289
2014-2015	-	261	254	515
2016-2017	-	263	268	531
2018-2019	-	262	272	534
2020	-	137	136	273
Total	2787	2390	1008	6185

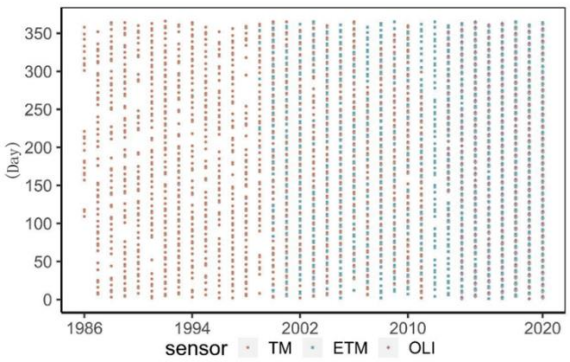

Figure 2.2 Temporal Distribution of Landsat Images

2.1.2 Used Landsat Collections for RSEI

In order to produce the high-quality result of the ecological index with multi-temporal data derived from Landsat Collections, a total of 704 scenes were used, as detailed in Table 2.2 below.

Table 2.2 Data used for RSEI

Dataset \ Year	1990	2005	2019
Landsat 5 Surface Reflectance Tier1 (LANDSAT/LT05/C01/T1_SR)	75	121	-
Landsat 8 Surface Reflectance Tier1 (LANDSAT/LC08/C01/T1_SR)	-	-	117
Landsat 5 TM Collection 1 Tier 1 TOA Reflectance (LANDSAT/LT05/C01/T1_TOA)	152	116	-
Landsat 8 Collection 1 Tier 1 TOA Reflectance (LANDSAT/LC08/C01/T1_TOA)	-	-	123

2.1.3 Precipitation Data

Climate Hazards Group InfraRed Precipitation with Station data (CHIRPS) monitored the precipitation changes in the study area from 1986 to 2020. This dataset is a 30+ year quasi-global rainfall dataset available since 1981, which incorporates 0.05-degree resolution satellite imagery with in-situ station data (Funk et al, 2015). In addition, we selected precipitation data from the China Meteorological Data Service Centre (CMDC: https://data.cma.cn/site/index.html) for two meteorological stations close to the northern boundary of the study area to check the precipitation status near the two northern areas with more and less precipitation, respectively.

2.1.4 NASADEM Dataset

The digital evaluation dataset used in this paper is NASADEM (NASA JPL, 2020), which associated products generated from the Shuttle Radar Topography Mission (SRTM) data, with improved accuracy by incorporating auxiliary data from ASTER GDEM, ICESat GLAS, and PRISM datasets. There are 15 scenes of digital evaluation data with a pixel size of 30 m exported from GEE.

2.2 Methods

2.2.1 Workflow Process

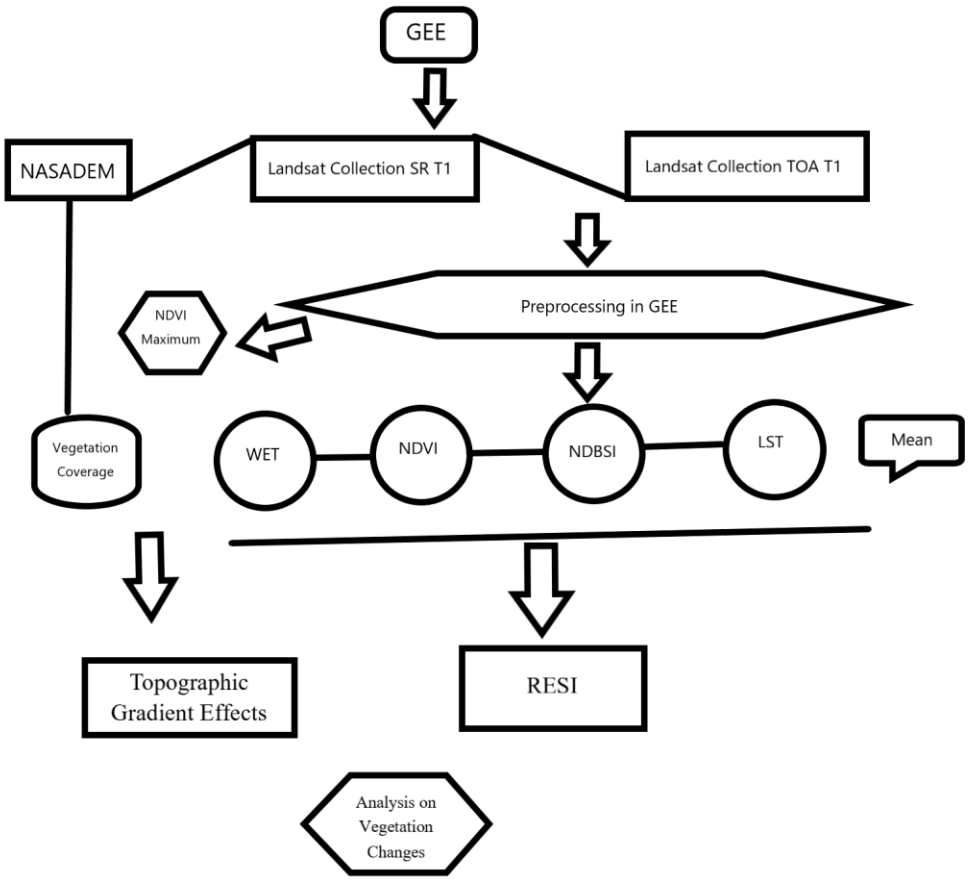

Figure 2.3 Workflow Process

Regarding the first part of this study, vegetation cover. First, the Landsat Collection SR Tier1 was pre-processed in GEE. Then the NDVI was calculated, followed by extracting the maximum values for every two years and exporting the images to be reclassified into ranges 0-0.3, 0.3-0.6, 0.6-1 for analyzing the changes in vegetation during 36-year, and also to overlay with the dem data for correlation analysis in 1988, 2008, 2020.

As for the second part, RSEI, the Landsat Collection TOA Tier1, and the Landsat Collection SR Tier1 were first pre-processed, then the mean values of WET, NDVI, LST, and NDBSI were calculated respectively in 1990, 2005, and 2019, and lastly, automatically and objectively weighted according to the nature of the data and the contribution of each indicator to PC1 of PCA method, avoiding any bias in the results caused by artificially determined weights.

2.2.2 Data Preprocessing

2.2.2.1 Data Processing Platform - GEE

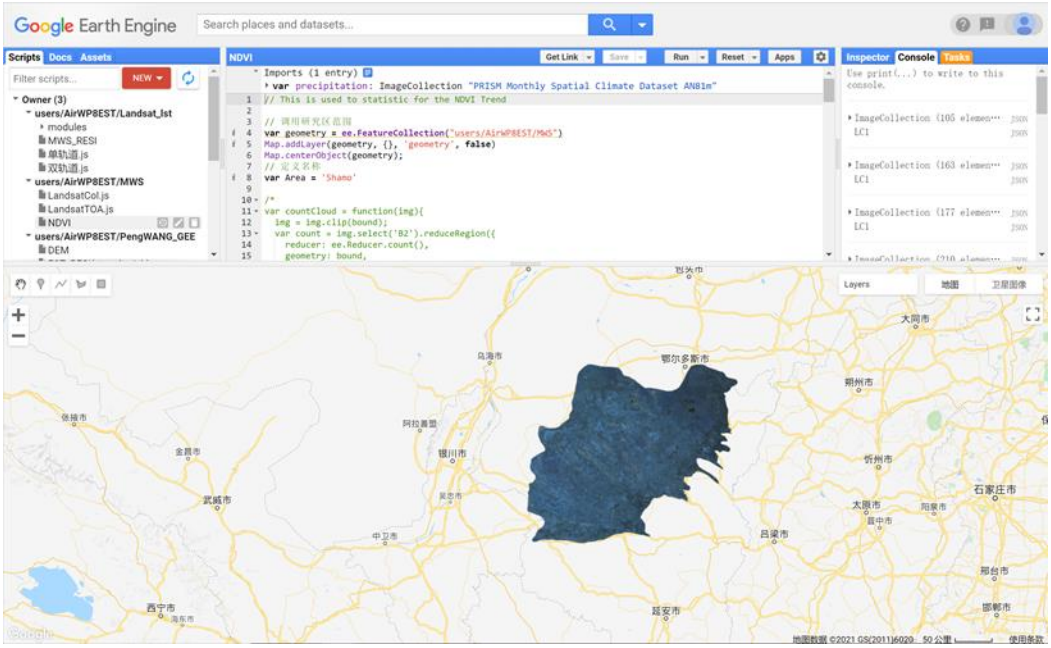

Figure 2.4 Interface of GEE Platform

Currently there are many tools used to process remote sensing images, such as the most popular and well known is the ENVI software, which is fee based at a very high cost. Also there are free software and tools, such as QGIS, GDAL, etc. A common feature of all these software and libraries is that they run locally, and their processing power is positively correlated with the local equipment, while GEE runs on Google Cloud, and its processing power is not limited by space or time. Since geographical data are often large and complicated to store, GEE provides a quickly accessible collection of ready-to-use data products. In addition, it is open and free to the public. as shown in Figure 2.5, We are able to import multiple datasets with thousands of images in GEE to perform operations simultaneously and obtain the required data efficiently. Figure 2.6 shows the code we used in our study to extract the maximum pixels per two years in the study area, which is difficult to achieve using conventional remote sensing software.

```
''
var LT4col = ee.ImageCollection('LANDSAT/LT04/C01/T1_TOA').select(rawVar1);
var LT5col = ee.ImageCollection('LANDSAT/LT05/C01/T1_TOA').select(rawVar1);
var LE7col = ee.ImageCollection('LANDSAT/LE07/C01/T1_TOA').select('B6_VCID_

var LC8col = ee.ImageCollection('LANDSAT/LC08/C01/T1_TOA').select(rawVar2,
//print(LC8col.first(),'LC8col')
//--------------- L8 to L7 HARMONIZATION FUNCTION ------------------------
```

Figure 2.5 Importing Landsat Collection in GEE

```
for (var y = 1986; y <= 2020; y = y+2){

  var LC1 = LC.filter(ee.Filter.calendarRange(y, y+1, 'year'))
  print(LC1, 'LC1')

  var NDVISR_img = LC1.select('ndvi')
                      .max()
                      .clip(geometry);

  Map.addLayer(LC1.median().clip(geometry),
               {min:0, max:4000},
               'Landsat_img')

  Map.addLayer(NDVISR_img, {min:-1,max:1}, 'NDVIImg');
```

Figure 2.6. Extracting Maximum Value of NDVI

2.2.2.2 Cloud Mask

The Landsat collection L1 T1 has been geometrically corrected, radiometric calibrated by the USGS (Masek, 2006) and processed with cloud mask based on the FMask algorithm (Foga et al., 2017; Zhu et al., 2015) . In particular, FMask (as shown in Figure 2.7) is the official USGS automated cloud detection algorithm for Landsat images using cloud matching techniques and cloud height iteration algorithms for cloud detection. After cloud detection by the Fmask algorithm, each image element of each scene has its corresponding image cloud flag, which are clear, water, cloud, cloud shadow and snow. In this paper, the cloud signatures of cloud, cloud shadow and snow are removed and all remaining clear image elements are used for subsequent studies.

```
// Define function to mask out clouds and cloud shadows
// landsat 5 and landsat 7
function cloudMaskL457(img) {
  var qa = img.select('pixel_qa');
  // If the cloud bit (5) is set and the cloud confider
  // or the cloud shadow bit is set (3), then it's a ba
  var cloud = qa.bitwiseAnd(1 << 5)
                .and(qa.bitwiseAnd(1 << 7))
                .or(qa.bitwiseAnd(1 << 3));
  // Remove edge pixels that don't occur in all bands
  var mask2 = img.mask().reduce(ee.Reducer.min());
  //print(mask2)
  return img.updateMask(cloud.not()).updateMask(mask2);
}
```

```
// landsat 8
function maskL8sr(img) {
  // Bits 3 and 5 are cloud shadow and cloud, respectively.
  var cloudShadowBitMask = (1 << 3);
  var cloudsBitMask = (1 << 5);
  // Get the pixel QA band.
  var qa = img.select('pixel_qa');
  // Both flags should be set to zero, indicating clear cor
  var mask = qa.bitwiseAnd(cloudShadowBitMask).eq(0)
               .and(qa.bitwiseAnd(cloudsBitMask).eq(0));
  return img.updateMask(mask);
}
```

Figure 2.7 Cloud Mask Code Used in GEE

2.2.2.3 Band Value Adjustment

Considering the system error caused by different TM, ETM+, and OLI sensors (Table 2.3), it is necessary to adjust the band value of different sensors. Roy et al. (2016) compared the band values of different sensors in Landsat. They proposed a set of linear adjustment formulas to ensure that LDCM data are sufficiently consistent with data from the earlier Landsat missions regarding acquisition geometry, calibration, coverage characteristics, spectral characteristics, output product quality. In this paper, the formulas (1) are used to linearly adjust the image band values of Landsat 8 OLI sensors.

$$\begin{cases} Blue: OLI = -0.0095 + 0.9785\ ETM +/TM \\ Green: OLI = -0.0016 + 0.9542\ ETM +/TM \\ Red: OLI = -0.0022 + 0.9825 ETM +/TM \\ NIR: OLI = -0.0021 + 1.0073\ ETM +/TM \\ SWIR1: OLI = -0.0030 + 1.0171\ ETM + /TM \\ SWIR2: OLI = 0.0029 + 0.9949\ ETM +/TM \end{cases} \quad (1)$$

Table 2.3 Landsat Bands Combination

Landsat-5 TM Bands (μm)			Landsat-7 ETM+ Band (μm)		Landsat-8 OLI and TIRS Bands (μm)		
					30 m Coastal/Aerosol	0.435 – 0.451	Band 1
Band 1	30 m Blue	0.45 – 0.52	30 m Blue	0.441 - 0.514	30 m Blue	0.452 – 0.512	Band 2
Band 2	30 m Green	0.52 - 0.60	30 m Green	0.519 – 0.601	30 m Green	0.533 – 0.590	Band 3
Band 3	30 m Red	0.63 - 0.69	30 m Red	0.631 – 0.692	30 m Red	0.636 – 0.673	Band 4
Band 4	30 m NIR	0.76 - 0.90	30 m NIR	0.772 – 0.898	30 m NIR	0.851 – 0.879	Band 5
Band 5	30 m SWIR-1	1.55 - 1.75	30 m SWIR-1	1.547 – 1.749	30 m SWIR-1	1.566 – 1.651	Band 6
Band 6	120m TIR	10.40 - 12.50	60 m TIR	10.31 – 12.36	100 m TIR-1	10.60 - 11.19	Band 10
					100 m TIR-2	11.50 – 12.51	Band 11
Band 7	30m SWIR-2	2.08 - 2.35	30 m SWIR-2	2.064 – 2.345	30 m SWIR-2	2.107 – 2.294	Band 7
Band 8			15 m Pan	0.515 – 0.896	15m Pan	0.503 – 0.676	Band 8

2.2.3 NDVI and Vegetation Coverage

Most vegetation data in research applications use vegetation indices derived from RS satellite images. The current number of vegetation indices recorded in the Index Database (IDB) is 67, including the Normalized Difference Vegetation Index (NDVI), Simple Ratio Vegetation Index (SR), Difference Vegetation Index (DVI), Soil-Adjusted Vegetation Index (SAVI), Global Environmental Monitoring Index (GEMI), Aerosol Free Vegetation Index (AFVI), Enhanced Vegetation Index (EVI), etc. (Pinty et al.,1992; Hou et al., 2013.) Differing vegetation indices may offer distinct advantages and have several limitations. For instance, a SAVI can avoid soil disturbances, and AFVI and EVI are better at resisting atmospheric disturbances, whereas the calculation of these indices requires more information on the parameters or bands to be known.

Following previous studies, NDVI is straightforward to calculate and reflects the condition of surface vegetation to a large extent. (Julien et al., 2009), Moreover, the significant relationship between NDVI and various valued vegetation characteristics such as Gross Primary Production (GPP), Fraction of Photosynthetically Active Radiation (FPAR), and Leaf Area Index (LAI), which can effectively reflect vegetation cover and photosynthetic (Hou et al., 2013).

NDVI is calculated with the following expression:

$$NDVI = \frac{\rho_{NIP} - \rho_{Red}}{\rho_{NIP} + \rho_{Red}} \quad (2)$$

where NIR is near-infrared light and Red is visible red light.

The vegetation index values are generally extracted from single view imagery in conventional vegetation cover studies and thresholds used to classify vegetation from non-vegetation. However, vegetation index values are usually negative in areas where after removing clouds, water, and snow by pre-processing, these areas are prone to errors in the classification process. In this paper, the maximum value is extracted from hundreds of images for each cycle, which also reduces errors such as those described above. In this paper, the time series vegetation index was constructed through the following steps:

(1) Divide 18 time periods with a biennial cycle;

(2) Calculated NDVI index of all images within 2 years, and the maximum value (or appropriate threshold value) of each pixel is selected as the NDVI value, so as to obtain the vegetation index.

(3) Obtain vegetation index of 18 time periods to establish time series vegetation index.

The value of NDVI here will invariably be between -1 and +1. Values between -1 and 0 indicate dead plants or inorganic matter such as rocks, roads, and houses. Live plants tend to fall between a value of 0 and 1 for NDVI, with 1 being the healthiest and 0 being the least healthy (As shown in Figure 2.8). Each pixel in an image can be identified with a single value.

Figure 2.8 NDVI plant health value (Source: Sentera)

According to the classification of vegetation range for monitoring the vegetation changes in Mu Us Sandy Land by Liu et al.(2009), In this paper, vegetation coverage was classified into three grades according to the NDVI value. NDVI value of low vegetation coverage ranged from 0.0 to 0.3, medium vegetation coverage ranged from 0.3 to 0.6, and high vegetation coverage ranged from 0.6 to 1.0.

This paper investigates the influence of topography on vegetation; we set the slope range at 60 degrees (Figure 2.9) to analyze the correlation between slope and vegetation. By overlapping vegetation cover data with dem data, we selected three areas (Figure

2.10) with different topography to observe the vegetation coverage change on different terrains.

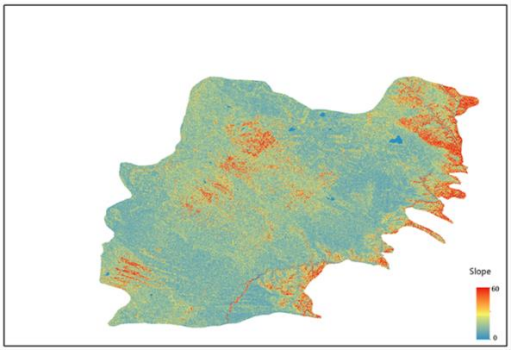

Figure 2.9 Slope of DEM

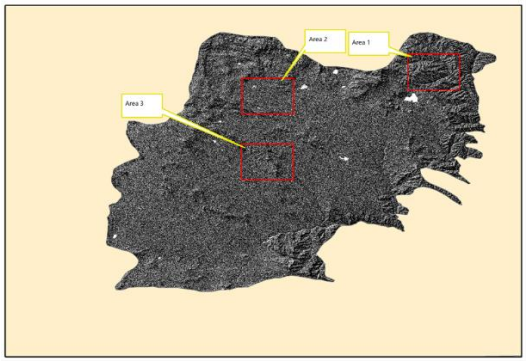

Figure 2.10 The Three Selected Areas

2.2.4. RSEI

The Remote Sensing Ecological Index (RSEI) is based on remote sensing technology, coupled with wetness, greenness, dryness and heat indexes directly related to the quality of ecological environment, which can visually and quickly evaluate the ecological environment, as a natural factor-based system for evaluating the quality of ecological environment. With the remote sensing image technology, the WET, NDVI (Gao et al., 2012), NDBSI (Xu, 2013; Wang et al., 2019) and LST can be obtained to represent the four ecological elements of moisture, greenness, dryness and heat respectively. There have been many studies using RSEI to assess the ecological environment (Li et al., 2020; Yang et al., 2019), most of which are urban-based. For example, the Guangdong-Hong Kong-Macao Greater Bay Area was used as the study area by Zheng (2019), who pointed out that the decline in ecological quality in the Guangdong-Hong Kong-Macao Greater Bay Area was closely related to the decline in vegetation cover and the increase in surface temperature.

As far as remote sensing technology is concerned, it can use thematic information enhancement techniques to extract information on these four important indicators from the various remote sensing image data, such as the vegetation index, surface temperature, and the humidity component of the tassel transformation to represent greenness, heat and humidity respectively. As buildings are an important part of the artificial ecosystem, the large number of impermeable surfaces replaces the original natural ecosystem of the ground, resulting in the 'drying out' of the ground. The bare soil index can therefore be used to represent the 'dryness'. In this way, the proposed remote sensing ecological index can be expressed as a function of these four indicators. As formula 3 and 4:

$$RSEI = f(G, W, T, D) \quad (3)$$

Defined by RS index:

$$RSEI = f(VI, WET, LST, NDBSI) \quad (4)$$

Where G is greenness, W is wetness, T is temperature and D is dryness.

(1) Wetness indicator

The tassel cap transform is an effective data compression and de-redundancy technique, and its brightness, greenness, and wetness components are directly related to the physical parameters of the ground surface; consequently, it has been widely used in ecological monitoring. The moisture component of this study is represented by the Wet, as it is closely related to the moisture content of the vegetation, water body, and soil. The wetness components of TM and OLI correspond to different calculation parameters and can be computed with formula 5:

$$\begin{cases} Wet\ (TM) = 0.0315\ \rho_1 + 0.2021\ \rho_2 + 0.3102\ \rho_3 + 0.1594\ \rho_4 - 0.6706\ \rho_5 - 0.6109\ \rho_7 \\ Wet\ (OLI) = 0.1511\ \rho_2 + 0.1973\ \rho_3 + 0.3283\ \rho_4 + 0.3407\rho_5 - 0.7117\ \rho_6 - 0.4559\ \rho_7 \end{cases} \quad (5)$$

(2) Heat indicator

$$L = gain * DN + bias \quad (6)$$

$$T = K_2 / \ln(K_1/L + 1) \quad (7)$$

Where K_1 and K_2 are calibration parameters, K_1 = 607.76 W m^{-2} $\mu m^{-1} sr^{-1}$ and K_2 = 1260.56 K if obtained from the TM, and K_1 = 774.89 W m^{-2} $\mu m^{-1} sr^{-1}$ and K_2 = 1321.08 K for the Thermal Infrared Sensor (TIRS) Band 10.

$$LST = T/[1 + (\lambda T/\rho) \ln \varepsilon] \quad (8)$$

λ is certer wavelength and ε is surface emissivity

(3) Dryness

The dryness of the surface soil is commonly calculated using the bare soil index (SI) in RS studies about desertification. Although the study area is a desert, taking into account that the part of the study area in Shaanxi Province has a relatively large amount of built-up land, which also contributes to the dryness of the ground surface. Therefore, this study used normalized difference built-up and bare-soil index (NDBSI), which is a combination of the SI and an anthropic index, the index-based built-up index (IBI) (Xu, 2017), to represent the dryness in the study area, as in formula 9.

$$NDBSI = (IBI + SI)/2 \quad (9)$$

$$IBI = 2\rho 5/(\rho_5 + \rho_4) - [\rho_4/(\rho_4 + \rho_3) + \rho_2/(\rho_2 + \rho_5)]/\{2\rho_5/(\rho_5 + \rho_4) + [(\rho_4/(\rho_4/(\rho_4 + \rho_3) + \rho_2/(\rho_2 + \rho_5)]\} \quad (10)$$

$$SI = [(\rho_5 + \rho_3) - (\rho_4 + \rho_1)]/[(\rho_5 + \rho_3) + (\rho_4 + \rho_1)] \quad (11)$$

In RSEI, the first principal component (PC1) of the Principal Component Analysis (PCA) method is used to integrate the 4 indicators. In this case, each indicator is automatically and objectively weighted according to the nature of the data and the contribution of each indicator to PC1, avoiding any bias in the results caused by artificially determined weights (Xu, 2013).

The RSEI was calculated as formula 12:

$$RSEI = PC1[f(NDVI, WET, NDBSI, LST)] \quad (12)$$

It is necessary to normalize each indicator before performing PCA, resulting in all of the values in the range from 0 to 1, normalization formula as follows:

$$NI_i = \frac{I_i - I_{min}}{I_{max} - I_{min}} \quad (13)$$

Where NI_i is the normalized value of a pixel, I_i is the value of a pixel, and I_{max} and I_{min} are the max and min values of a pixel, respectively.

The value of RSEI is between 0 and 1. The closer the RSEI value is to 1, the better the ecological condition is, and vice versa. Based on previous studies, we classify values into five grades in equal intervals: 1 – poor (0-0.2), 2 – fair (0.2-0.4), 3 – moderate (0.4-0.6), 4 – good (0.6-0.8), 5 – excellent (0.8-1.0).

3. Evolution and Analysis of Vegetation Coverage

3.1 Analysis of Temporal and Spatial Evolution on Characteristics of Vegetation Coverage Changes Since 1986

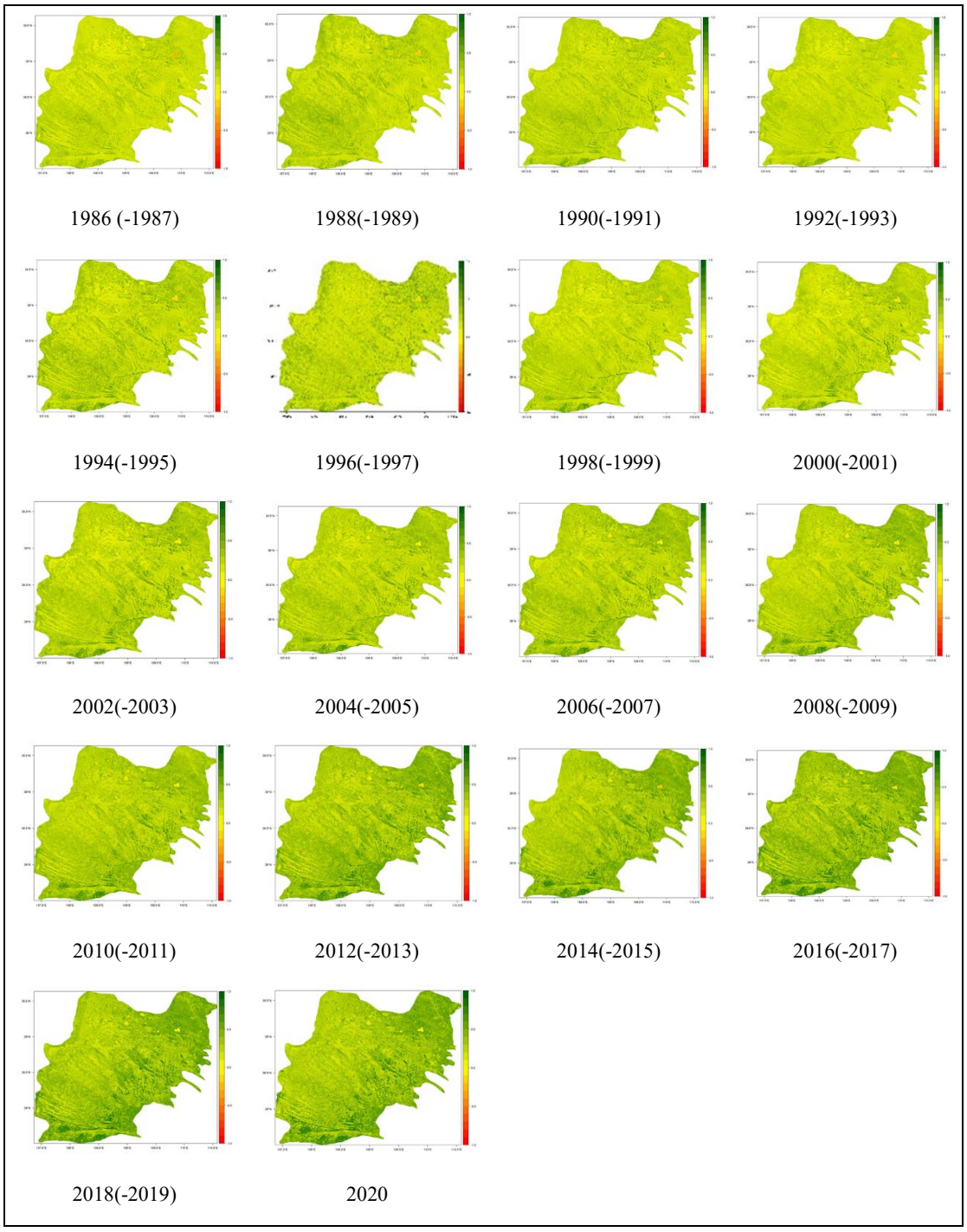

Figure 3.1.1 NDVI-based vegetation changes from 1986 to 2020

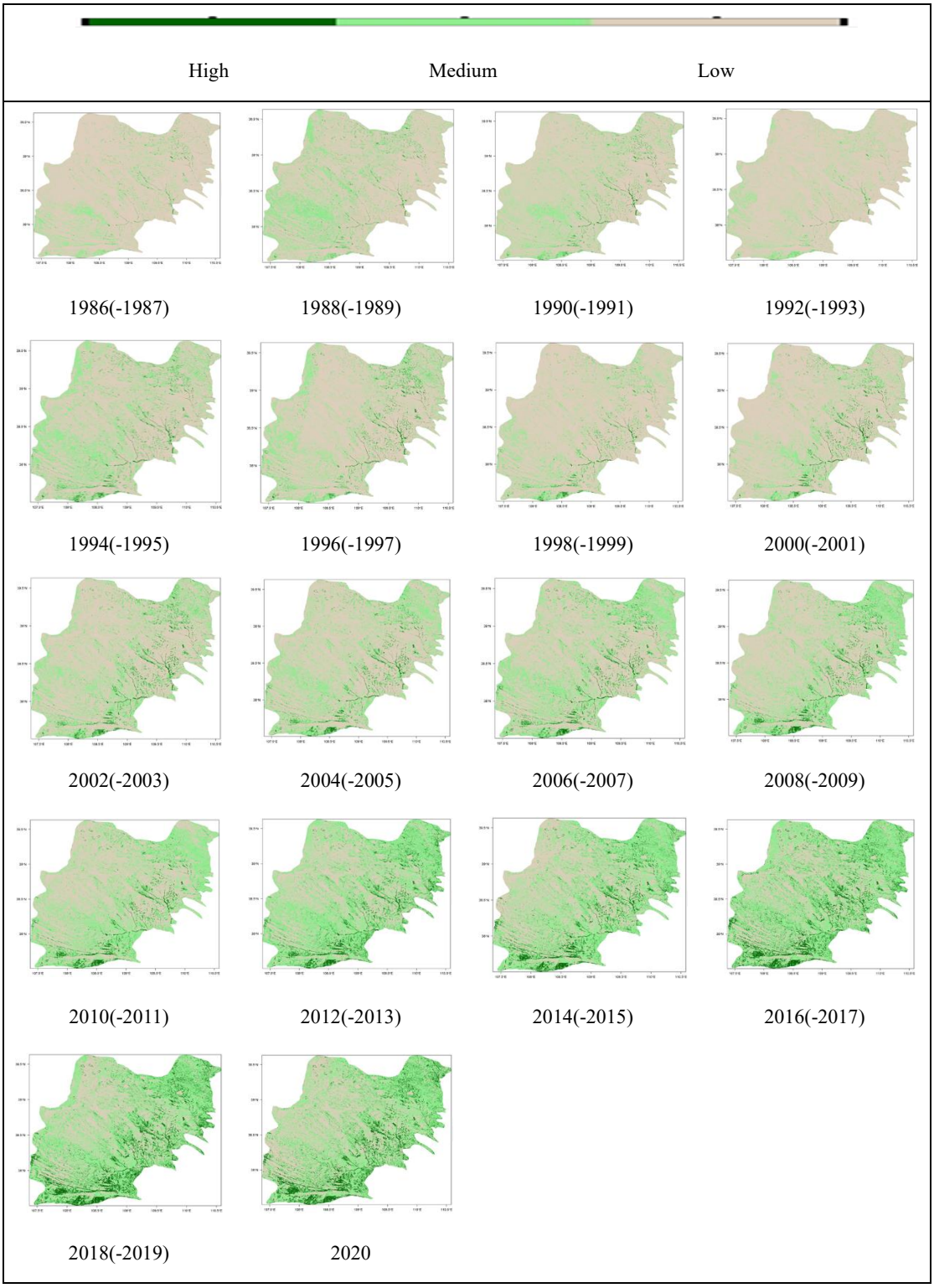

Figure 3.2 Vegetation Coverage Changes from 1986 to 2020

As shown in Figure 3.2, the area of vegetation in the north-eastern part of Mu Us Sandy Land generally appears to be steadily increasing with each cycle, with the quality of the vegetation practically being medium until 2020. Only slightly visible moderate vegetation cover was observed in the central, northern, and western regions of the study area in 2012, compared to these periods from 2014 to 2020, without any significant

increase in the extent of cover in these regions up to 2020. A small cover of high vegetation occurs on the southern edge in 1994, and by 2020 this area is covered mainly by high and medium vegetation, while this is also the main concentration of high vegetation coverage during all the study cycles. Notwithstanding the apparent overall increase in vegetation cover, there are still large areas where the vegetation is in a precarious state of growth, while the quality of vegetation growth has not improved significantly.

According to the hierarchical classification method of vegetation coverage grade, this paper has classified the time series vegetation index and has received the classification results of time series vegetation coverage since 1986. After analyzing the vegetation coverage in the research area since 1986, we found that in the early stage, the vegetation coverage was mainly low, followed by the medium vegetation coverage, and the high vegetation coverage was less; in the later period, the low vegetation coverage decreased significantly, while the medium and high vegetation coverage increased significantly. Since 1986, the vegetation index in the Mu Us Sand Land has maintained a continuous upward trend, with the median values increasing from 0.18 (1986) - 0.34 (2020) and annual values increasing from 0.20 (1986) - 0.38 (2020) in 2020 (Table 3.1),

Table 3.1 Vegetation index of time series NDVI from 1986-2020

Stage	*Year*	*Median value*	*Annual average*
Stage 1	1986	0.18	0.20
	1988	0.20	0.23
	1990	0.21	0.23
	1992	0.18	0.21
	1994	0.22	0.25
	1996	0.21	0.24
	1998	0.20	0.22
	2000	0.20	0.23
	Average	**0.21**	**0.23**
Stage 2	2002	0.24	0.26
	2004	0.25	0.27
	2006	0.26	0.28
	2008	0.26	0.29
	2010	0.29	0.31
	2012	0.34	0.36
	Average	**0.27**	**0.29**
Stage 3	2014	0.32	0.35
	2016	0.37	0.39
	2018	0.36	0.39
	2020	0.34	0.38
	Average	**0.35**	**0.38**

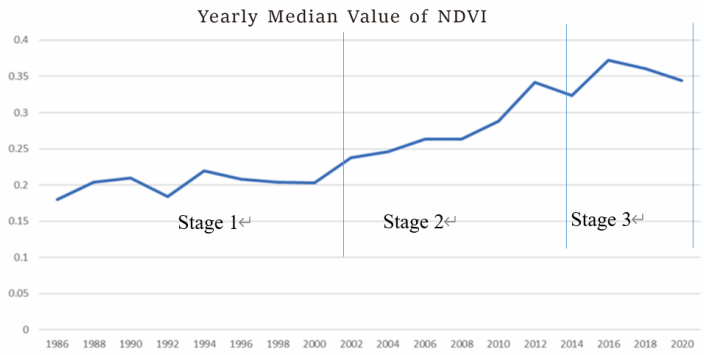

Figure 3.3 median value of time series NDVI from 1986 to 2020

Table 3.2 Classification results of time series vegetation coverage from 1986 to 2020

Stage 1									
Year	1986	1988	1990	1992	1994	1996	1998	2000	**Average**
Low coverage	87.00%	74.50%	77.70%	86.70%	69.60%	76.20%	82.70%	80.10%	**78.20%**
Medium coverage	12.30%	23.90%	20.90%	12.90%	28.10%	21.70%	15.90%	17.90%	**20.20%**
High coverage	0.70%	1.60%	1.40%	0.40%	2.30%	2.10%	1.40%	2.00%	**1.70%**
Stage 2									
Year	2002	2004	2006	2008	2010	2012			
Low coverage	68.80%	67.80%	61.80%	61.30%	54.20%	38.30%			**58.70%**
Medium coverage	28.20%	29.50%	34.70%	35.10%	42.10%	54.70%			**37.40%**
High coverage	3.00%	2.80%	3.40%	3.60%	3.70%	7.00%			**3.90%**
Stage 3									
Year	2014	2016	2018	2020					
Low coverage	42.90%	31.60%	34.10%	38.30%					**36.70%**
Medium coverage	49.80%	57.70%	54.40%	50.70%					**53.10%**
High coverage	7.20%	10.70%	11.50%	11.00%					**10.10%**

It can be learned that there are 3 stages (Figure 3.3) of vegetation index change in the Mu Us Sand Land since 1986:

(1)Stage 1(1986-2000): the NDVI value was relatively stable, the median NDVI value was basically maintained between 0.18 and 0.22, and the average value was 0.21;

(2)Stage 2(2002-2012): during this period, the median NDVI kept increasing significantly year by year, from 0.24 in 2004 to 0.29 in 2010;

(3)Stage 3(2014-nowadays): the NDVI values are stable, and maintain a relatively high

value between 0.32-0.37, with the average value of 0.35.

In this paper, the vegetation coverage classification method was adopted to classify the NDVI annual median value according to the threshold value, and obtained results of time series vegetation coverage from 1986 to 2020 (Table 3.2 and Figure 3.4).

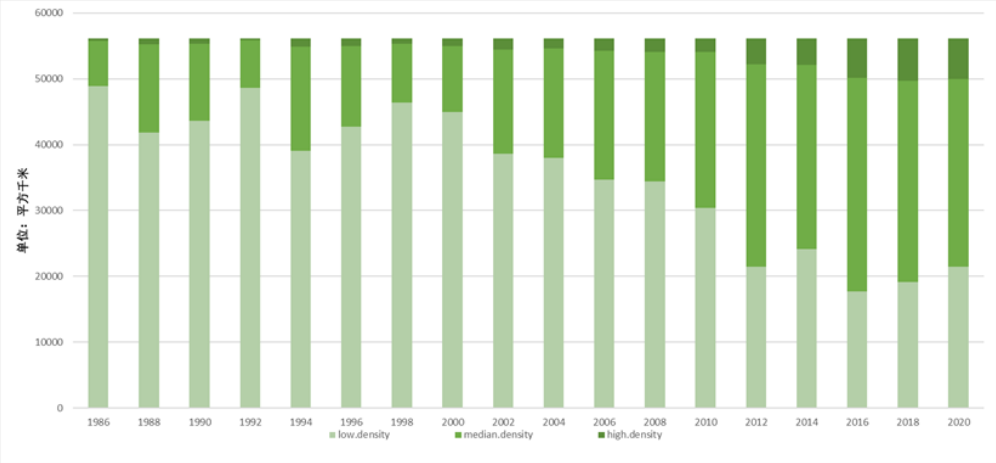

Figure 3.4 Curve graph of time series vegetation coverage classification from 1986-2020

Thus, the changes of vegetation coverage since 1986 are as follows:

(1) Stage 1(1986-2020): vegetation coverage was mainly low, accounting for about 78.2%, the medium coverage was slightly changed, accounting for about 20.0%, and there was few high coverage, accounting for about 1.7%.

(2) Stage 2 (2000-2012): the low vegetation coverage gradually decreased from 68.8% in 2002 to 38.3% in 2012; the medium coverage significantly increased from 28.2% in 2002 to 54.7% in 2012; the high coverage slightly increased from 3.0% in 2002 to 3.9% in 2012;

(3) Stage 3: Since 2014, on the basis of relatively stable low coverage (36.7%) and medium coverage (53.1%), the high vegetation coverage increased significantly, the average annual coverage has rosen from 7.2 percent in 2014 to 11.0 percent in 2020;

(4) In 1986, the study area was in the stage of desertification, and its vegetation coverage was mainly low, accounting for 87% of the total study area, while by 2020, the desertification control in the study area has achieved remarkable results. The vegetation coverage is mainly medium and high, and the low coverage has been reduced to about 30%.

3.2 The Effect of Topographic Gradient on Vegetation Coverage

Combined with the digital elevation model (DEM) of Mu Us Sand Land, 1988, 2008 and 2020 are selected as the typical years of the 3 stages according to the terrain changes. 3 typical areas (area 1 has a large topographic change, area 2 has the gentlest topographic change, and area 3 has a medium topographic change) are selected to analyze the vegetation coverage. The vegetation coverage changes are shown in Figure 3.5-3.7.

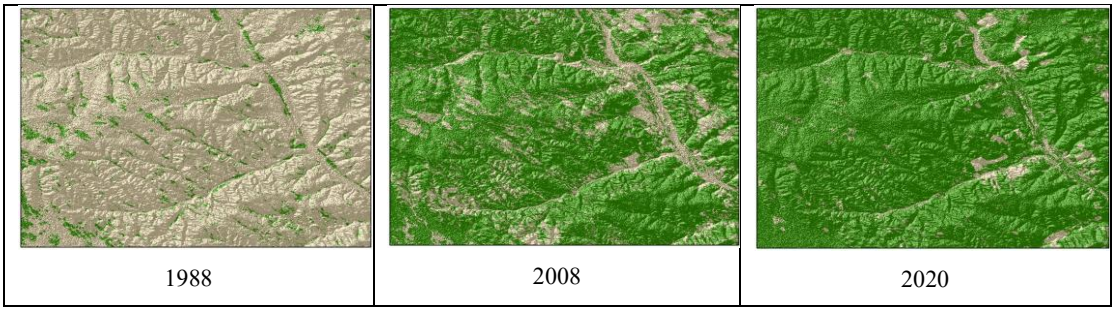

Figure 3.5 Vegetation coverage changes in area 1(1988, 2008 and 2020)

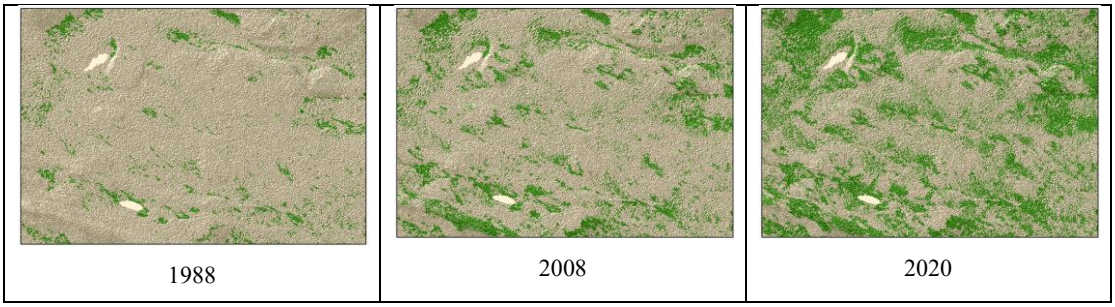

Figure 3.6 Vegetation coverage changes in area 2(1988, 2008 and 2020)

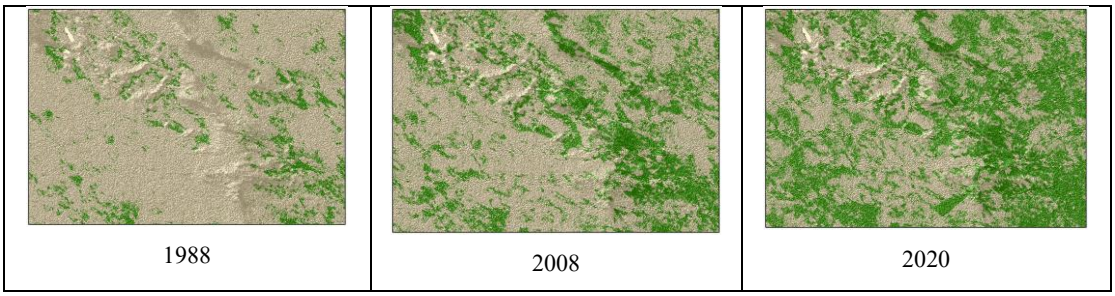

Figure 3.7 Vegetation coverage changes in area 3(1988, 2008 and 2020)

As can be seen from the figures above: in area 1, the topographical changes greatly and the vegetation coverage increases rapidly, the vegetation coverage was mainly low in 1988 and increased significantly in 2008, while in 2020, the vegetation coverage was mainly high; in area 2, with gentle terrain and minimal topographical changes, the growth of vegetation coverage is very slow, from 1988 to 2008, although the high coverage increased slightly, area 2 was still dominated by low coverage, while in 2020, the high coverage increased significantly; both topographical changes and growth rate of area 3 are between area n1 and area 2. It can be seen that the vegetation coverage change is closely related to topography. The larger the topographical change, the faster the vegetation grows; the smaller the topographical change, the slower the vegetation

grows.

Combined with slope data of Mu Us Sand Land, the vegetation index of the study area in 3 typical years was analyzed and obtained the correlogram of vegetation index and slope (Figure 3.8).

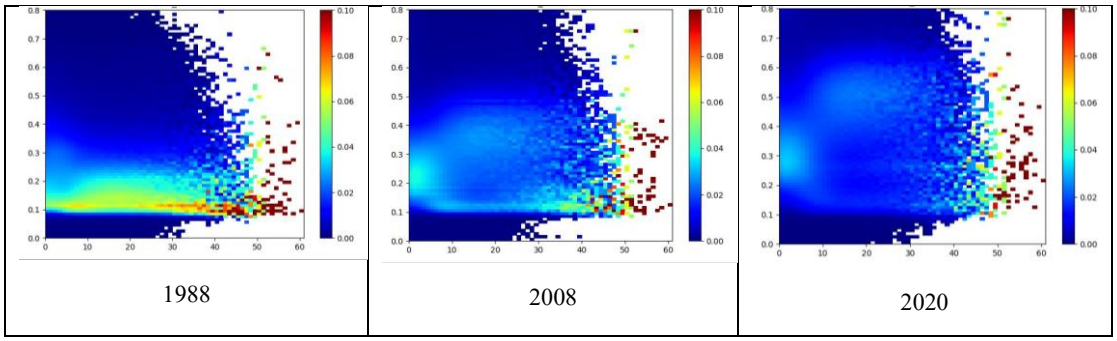

Figure 3.8 Correlogram of vegetation index and slope(1988, 2008, 2020)

We can learn that when the NDVI index and the process of vegetation coverage in an overall upward trend, they are related with slope in a certain degree:

- At the range of 1-10 degree: the index was mainly distributed between 0.1-0.2 in 1988,0.2-0.3 in 2008 and around 0.3 in 2020; the growth rate of vegetation index in this region was very slow, and its vegetation coverage was still mainly low and medium in 2020.
- At the range of 10-30 degree: the index was mainly distributed between 0.1-0.2 in 1988, 0.3-0.4 in 2008 and around 0.5 in 2020; the growth rate of vegetation index increased rapidly in this region, and its vegetation coverage was mainly medium, while the high vegetation coverage has increased significantly.

3.3 Analysis on RSEI-based Ecological Monitoring

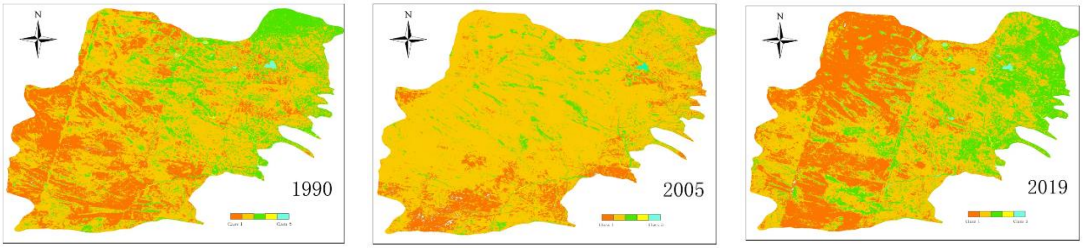

Figure 3.9 Spatial distribution of different RSEI quality grades in 1990, 2005, 2019.

RSEI	1990		2005		2019	
	km^2	（%）	km^2	%	km^2	%
1：（0-0.2）	14055.2	23.06	6146.68	10.96	17465	31.15
2：（0.2-0.4）	32540	60.02	46193.3	82.39	26681.7	47.59
3：（0.4-0.6）	9048.63	16.14	3509.46	6.25	11177.8	19.94
4：（0.6-0.8）	335.16	0.63	147.56	0.26	580.9	1.04
5：（0.8-1）	85.01	0.15	67	0.14	158.6	0.28
Amount	56064	100	56064	100	56064	100

1 – poor (0-0.2), 2 – fair (0.2-0.4), 3 – moderate (0.4-0.6), 4 – good (0.6-0.8), 5 – excellent (0.8-1.0)

Table3.3 The changes of RSEI in Mu Us Sandy Land

Observing the ecological condition as a whole over three years, it is Observing the ecological condition as a whole over these three years, it is clear as we see that nearly all of the areas are in grades 1, 2, and 3, and the areas that can meet the ‘good’ and ‘excellent’ criteria are barely visible (Figure 3.9).Therefore, in our opinion, the current ecological environment of Mu Us Sandy Land is fragile evaluated based on the RSEI. In 1990, a portion of the Ejin Horo Banner area located in the northeastern part of the Mu Us Sandy Land showed an ecological condition of moderate class, most of the areas of the Uxin Banner, Yulin City, and Shenmu County ranged from 0.2 to 0.4, while the remaining areas suffered from a severely poor ecological condition. In 2005 the ecological condition deteriorated significantly in the area of Ejin Horo Banner and Hengshan county located in Mu Us Sandy Land, while the ecology of Otog Front Banner, Jingbian County, parts of Uxin Banner, and a minor southern part of Yulin city improved to moderate class, with no significant local changes in the rest of study area (Figure 3.10 A). Combining the vegetation cover from 2014 and 2015, we found an increase in moderate vegetation cover where the Ejin Horo Banner was ecologically improved. As of 2019, an improved ecological situation had only been observed in Yulin and Shenmu. Compared to 1990, we found a significant reversal between the eastern and western parts of the study area over the two cycles (Figure 3.10 B); in 2019, there is an 8.09% degradation of the RSEI to class 1, a 12.43% drop in class 2, a 3.8% upturn in class 3 and only a very slightly improved in the ecological condition in classes

4 and 5.

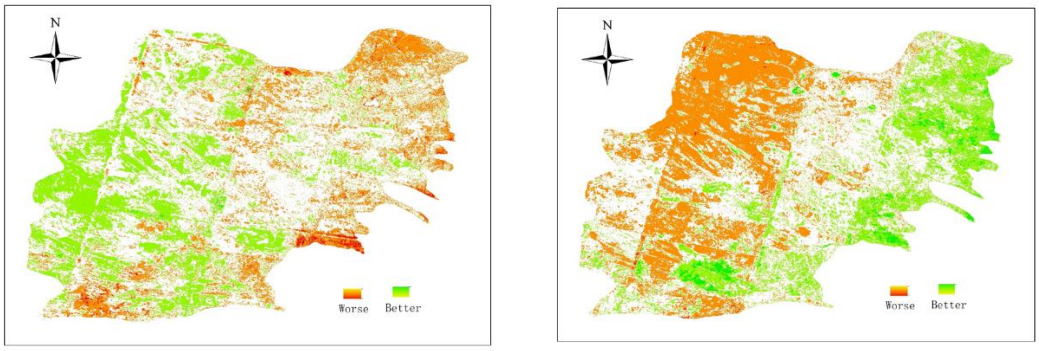

A. Changes between 1990 and 2005 B. Changes between 2005 and 2019

Figure 3.10 Change magnitude map of RSEI

	NDVI	WET	NDBSI	LST	RSEI
NDVI	1				
WET	0.325335	1			
NDBSI	-0.51884	-0.51678	1		
LST	-0.13277	-0.51678	0.517493	1	
RSEI	0.133269	0.517493	-0.41571	-0.9986	1

Table 3.4 Correlation matrix in 1990

	NDVI	WET	NDBSI	LST	RSEI
NDVI	1				
WET	0.516991	1			
NDBSI	-0.53648	-0.75811	1		
LST	-0.11393	-0.39471	0.440048	1	
RSEI	0.117804	0.400099	-0.44695	-0.99857	1

Table 3.5 Correlation matrix in 2005

	NDVI	WET	NDBSI	LST	RSEI
NDVI	1				
WET	0.540823	1			
NDBSI	-0.6427	-0.83434	1		
LST	-0.39666	-0.62425	0.59805	1	
RSEI	0.396562	0.628834	-0.5985	-0.9997	1

Table 3.6 Correlation matrix in 2019

Combining Table 3.4 and 3.6, we find that an increase in vegetation correlates with an increase in RSEI. The negative correlation between RSEI and Surface temperature is consistently high. And the increase in vegetation will reduce the surface temperature and dryness to some extent, while it enhances the humidity. In 2015, though a very slight moderate vegetation increase in the study area, the loss of WET drove a reduction in NDVI's correlation with RSEI.

3.4 Summary of Analysis

This chapter is presented calculated time-series NDVI vegetation index by using the long-term series Landsat remote sensing image data with a period of 2 years; dividing the NDVI values into three grades according to the thresholds: low vegetation coverage (0.0 ~ 0.3), medium vegetation coverage (0.3 ~ 0.6) and high vegetation coverage (0.6 ~ 1.0), analyzing vegetation coverage grade since 1986. Then the vegetation results for the three years 1988, 2008, and 2020 were selected and combined DEM to conduct researches on the impact of topography on vegetation coverage and correlation analysis between slope (range 0-60 degrees) and vegetation coverage. Furthermore, 704 scenes Landsat images were processed for monitoring changes in ecological conditions in 1900, 2005, and 2019 based on the RSEL's ecological index combining the four indicators LST, WET, NDVI, and NDBSI; the normalized results were classified into five classes: 1 – poor (0-0.2), 2 – fair (0.2-0.4), 3 – moderate (0.4-0.6), 4 – good (0.6-0.8), 5 – excellent (0.8-1.0). The results are as follows:

(1) Since 1986, there are 3 periods of the vegetation coverage in Mu Us Sand Land: Period 1 – severe desertification(1986 - 2000), Period 2 – recovery(2002 - 2012), Period 3 – stationary(2014 - nowadays)

(2) Although vegetation cover in the study area increased significantly from 1986 to 2020, the high vegetation cover is mainly on the southern edge and southeast. Growth in vegetation cover has been steady in the east and southeast, with mainly medium vegetation. Elsewhere the vegetation cover shows improvement, but the quality of growth us not satisfactory.

(3) the vegetation coverage index processes are as follows:

- Stage 1(1986 - 2000), the NDVI value was generally stable with slight changes
- Stage 2 (2002 - 2012), the NDVI value kept increasing significantly.
- Stage 3(2014 - nowadays), NDVI was stable again and maintained a relatively high value.

(4) the vegetation coverage grade processes are as follows:

- Stage 1(1986-2000): the vegetation coverage during this period was very low, and was mainly low vegetation coverage, followed by medium, and high vegetation coverage.
- Stage 2(2002-2012): the low vegetation coverage gradually decreased, the medium coverage gradually increased, and the high coverage slowly increased.
- Stage 3(2014 – nowadays): the low vegetation coverage rate stably decreased, the

medium coverage was relatively stable, and the high coverage increased significantly.

(5) In 1986, the study area was in desertification stage, and its vegetation coverage was mainly low, accounting for 87% of the total study area. By 2020, the desertification control has achieved remarkable results. The low vegetation coverage is mainly replaced by medium and high vegetation coverage, and been reduced to about 30%.

(6) Topography can affect the evolution process of vegetation coverage in a certain degree. Topographic relief areas provide vegetation better growing habitats and the vegetation coverage rate changes rapidly from low to high. While in flat terrain, the growing habitats are worse, and the vegetation coverage rate here changes very slowly.

(7) When the NDVI index and the process of vegetation coverage in an overall upward trend, they are related with slope in a certain degree: at the range of 1-10 degree, the growth rate of vegetation index is very slow, up to 2020, the index has been mainly distributed around 0.3, and is mainly low and medium vegetation coverage; in the range of 10-30 degree, the growth rate increased rapidly, up to 2020, it has been mainly distributed around 0.5, and the vegetation coverage is mainly medium, with significant increase of high vegetation coverage;

(8) The desertification control in the study area has achieved remarkable results. In 1986, the study area was in desertification stage, and the vegetation coverage was mainly low. By 2020, the vegetation coverage had been greatly improved, and the vegetation coverage was mainly medium and high.

(9) The comprehensive eco-environment appraisal index has gone up, with the improvement of vegetation coverage; Moreover, the increase of vegetation coverage partly results in the increase in Wet and the decrease in LST and NDBSI. NDVI is only an element of RSEI but not a decisive factor that can change RSEI, an increase in NDVI without a substantial change in quality and quantity might not significantly impact ecological change.

In broad terms, as of 2019, only the areas of Yulin and Shenmu located within the Mu Us Sandy Land have seen a steady increase in vegetation along with ecological improvements, but both are at a moderate level, with vegetation cover and the ecological index falling far short of the optimal range.

4. Discussion

Although numerous people in various countries have studied deserts for a long time and established corresponding research systems and evaluation indicators, there is still a lack of an accepted evaluation indicator worldwide. The causes of desertification are mainly human factors and natural conditions. Differences in geographical location and climatic conditions can directly affect deserts by forming different deserts to different degrees. Contrary to the familiar Sahara Desert, the climatic conditions of the Mu Us Sandy Land are distinctly different. With relatively abundant annual rainfall decreasing from the northeast, where the precipitation is about 600 mm, to the southwest, where it falls to 300 mm. Meanwhile, the average annual temperature ranges from 6.78 to 10.66°C, with an average of -9.5 to -12°C in January and 22 to 24°C in July. Drivers affecting desert areas can be varied from region to region so developing a universally accepted system for assessing deserts worldwide is exceptionally challenging. In remote sensing, analyzing the desertification issue through remote sensing technology is still in the exploratory stage, and no real mature and trustworthy methods available at the moment. In arid and semi-arid areas with sparse vegetation and highly heterogeneous surfaces, determining the appropriate vegetation index is a key for detecting vegetation change through remote sensing. Gao et al. (2006) compared the NDVI, SAVI, MSAVI, and GEMI for monitoring vegetation change in arid and semi-arid areas, indicating that NDVI-based extraction of low vegetation cover produces the best outcome arid and semi-areas. We, therefore, used NDVI in this study to calculate the vegetation index of the study area. Thus, in this paper, the primary factors for evaluating desertification status in the study area are vegetation cover and ecological indicators, but whether these two indicators alone can fully reflect desertification status is still to be proven. For this study, we referred to some of the previous literature on the Mu Us Sandy Land. We found that the boundaries of their research area are almost non-uniform; the boundary data used in this study were also produced by ourselves according to the actual use of the land. Liu et al. (2009) detected the dynamic change of vegetation coverage of Mu Us Sandy Land from 1990 to 2007 using the overlay of two TM images of the vegetation bloom period during August to September. The area of the Mu Us Sandy Land in Liu et al. (2009) study, excluding the Otog Banner and part of the Uxin Banner, is only 34490.2392km^2, which is nearly 9000km^2 less than our present study. Even though we used identical data processing formulae and statistical methods, their numerical results on vegetation growth were much higher than our results. Due to the missing parts of their study, Otog Banner and Uxin Banner were the principal distribution areas of low vegetation, in cases when the original pixel extracted values should have been lower than our current study, as shown in the table below.

Annual changes rates 1990-2007			
VC Classification	Liu et al., 2009	Our study results	Our study results 1986-2020
Low Coverage	-0.048%	-0.99375%	-1.3528%
Medium Coverage	3,91%	0.8625%	1.0667%
High Coverage	3.48%	0.125%	0.64375%

Then we compared the study result with that by Qiu et al.(2019) monitoring vegetation change in the Mu Us Sandy Land from 2000 to 2015; in their case, we had a similar study boundary. However, he used a dataset containing both NDVI and EVI layers of the MOD13 product for the vegetation bloom period covering July to August. In our study, to ensure the quality of the pixel values, the highest values from the Landsat collection were derived and averaged for every two years. In the Qiu et al. (2109) study, the mean values from July to August of each year in the MOD13 product were derived and averaged. Then in this comparison, I calculated the average values of each of their two years to compare with our results. Since they only had 2015 values without 2016, we did not use our average value between 2015 and 2016 for comparison to ensure validity.

Average NDVI in Mu Us Sandy Land 2000-2014								
Years	2000	2002	2004	2006	2008	2010	2012	2014
Our Results	0.23	0.26	0.27	0.28	0.29	0.31	0.36	0.35
Qiu et al., 2019	0.20	0.26	0.26	0.25	0.27	0.29	0.33	0.28

On comparison, one finds that our values are a little higher at all times except 2006 when they are the same, but the difference between the values is not significant due to the high quality of their data products. Nevertheless, in principle it makes no sense for me to make a side-by-side comparison like this using maximum and mean values based on different satellite data. In the future, if we sought to verify the quality of the MOD13 product data, perhaps we could extract mean values from our dataset for comparison.

Presently the DEM data we use is limited as in this study; we used the only data available for 2010. For desert studies, many research scholars do fieldwork to collect data. However, many field trips are still inaccurate in capturing the actual situation of shifting sand dunes. The literature on dynamics monitoring in the Taklamakan, one of the most shifting dunes in China, and the Horqin Desert (Duan, 2013), a similar environment to the Mu Us Sandy Land, have integrated DEM to analyze land

degradation processes. We, therefore, apply DEM data to the analysis of vegetation cover in this study. Although we indicate topographic relief areas provide vegetation better growing habitats and the vegetation coverage rate changes rapidly from low to high in this study result, we consider this result to be a coincidental phenomenon. The growth of vegetation may be more strongly related to regional climatic conditions or the presence of soils, such as wind. Zhang et al. (2020) carried out 'vegetation rehabilitation in the Mu Us Sandy Land primarily affected by wind strength changes rather than other climates variables...and lowering of dune and increasing of vegetation arising from the decreasing wind strength. '

The RSEI, as applied in this paper, is commonly used to evaluate urban ecological conditions; we have not found cases where this index has been in use for analyzing desert or arid regions. However, by comparing 1990 and 2019, we consider that this index is still relatively effective for analyzing ecological problems in desert areas. In the future, we may try to improve the results by replacing the indicator calculation, such as LST. It is certainly not enough to rely only on these four indicators for ecosystem assessment, requiring an in-depth inquiry.

5. Conclusion and Expectation

This paper adopted the full-time Landsat series of remote sensing data (6185 in total) to create long-term series of NDVI vegetation index in 2 years from 1986 to 2020, and reclassifying NDVI into three grades by the threshold values: low vegetation coverage (0.0 ~ 0.3), medium vegetation coverage (0.3 ~ 0.6) and high vegetation coverage (0.6 ~ 1.0). Afterward, three years' vegetation results, 1988, 2008, and 2020, were selected to study the effect of topography on vegetation cover and the correlation analysis between slope (range 0-60 degrees) and vegetation cover in combination with DEM. Furthermore, 704 scenes Landsat images were manipulated for monitoring changes in ecological conditions in 1900, 2005, and 2019 based on the RSEL's ecological index combining the four indicators LST, WET, NDVI, and NDBSI; the normalized results were classified into five classes: 1 – poor (0-0.2), 2 – fair (0.2-0.4), 3 – moderate (0.4-0.6), 4 – good (0.6-0.8), 5 – excellent (0.8-1.0). The main conclusions are as follows:

(1) There is relatively abundant precipitation in Mu Us Sand Land, which is conducive to vegetation;

(2) Since 1986, there are 3 periods of the vegetation coverage in Mu Us Sand Land: Period 1 – severe desertification(1986 - 2000), the NDVI value was stable, and the vegetation coverage during this period was very low, and was mainly low vegetation coverage, followed by medium, and high vegetation coverage; Period 2 – recovery(2002 - 2012), the NDVI value kept increasing significantly, the low vegetation coverage gradually decreased, the medium coverage gradually increased, and the high coverage slowly increased; Period 3 – stationary(2014 - 2020), NDVI was stable again and maintained a relatively high value, while the low vegetation coverage rate stably decreased, the medium coverage was relatively stable, and the high coverage increased significantly.

(3) Topography can affect the evolution process of vegetation coverage in a certain degree. Topographic relief areas provide vegetation better growing habitats and the vegetation coverage rate changes rapidly from low to high. While in flat terrain, the growing habitats are worse, and the vegetation coverage rate here changes very slowly.

(4) When the NDVI index and the process of vegetation coverage in an overall upward trend, they are related with slope in a certain degree: at the range of 1-10 degree, the growth rate of vegetation index is very slow, up to 2020, the index has been mainly distributed around 0.3,; in the range of 10-30 degree, the growth rate increased rapidly, up to 2020, it has been mainly distributed around 0.5;

(5) The 36 years' desertification control in the study area has achieved remarkable results. In 1986, the study area was desertification stage, and the vegetation coverage was mainly low. By 2020, the vegetation coverage had been greatly improved, and the vegetation coverage was mainly medium and high.

(6) The vegetation growth has improved the ecology of the study area to some extent, but the specific causes of the ecological deterioration in 2005 we have no way of making a judgement based on the results alone and will need to explore other years on a case by case basis at a later date.

(7) The spatial distribution of the ecological index in 1990, 2005, and2019 is overwhelmingly in class 1, class 2, and class 3, resulting in a relatively fragile ecology for the study area as a whole, with Yulin city and Shenmu county showing fairly positive ecological trends in comparison.

(8) Considerable positive correlations between NDVI and Wet and positive correlations between NDVI and RSEI were found, with negative correlation indicators between NDVI and either LST or NDBSI increasing at a similar rate as the correlation between NDVI and RSEI increased.

In this paper, an automatic extraction method of vegetation index with high spatiotemporal resolution is established, which makes up for the shortcomings of conventional research methods such as low monitoring frequency, low automation level and so on. Due to the limitation of time, climate change and other conditions, conventional research methods usually select remote sensing images of sparse phase for processing and analysis, which cannot capture subtle changes of vegetation index. This paper makes full use of all-time series Landsat remote sensing images with a total of 6185 scenes, which can accurately identify subtle spatiotemporal characteristics of vegetation change in the Mu Us Sand Land. This study has calculated the time series NDVI vegetation index by using the long-term Landsat series of remote sensing data for 2 years. Due to the uneven spatiotemporal distribution of Landsat satellite remote sensing image data, the accuracy is still insufficient. Further studies can explore and combine more high-resolution remote sensing images as data sources to improve the accuracy of the evolution process of vegetation coverage. The RSEI is an index initially designed for the analysis of urban ecosystems. With no background on the use of this index to analyze ecological conditions in desert areas, an attempt was made in this study to use this index to investigate the study area. As only three years were chosen, it was not possible to capture the general overall ecological trends in the study area over 36 years, and to demonstrate the efficiency of this index when applied to desert areas; we would hope to have a further opportunity in the future to try to study the application of relevant indexes in this type of area.

Kokkuvõte

Magistritöö teema: Maowusu kõrbe haljastamise tuvastamine kaugseire abil

Kõrbestumine on muutunud rahvusvaheliselt ühiskonna jaoks keskseks probleemiks, mis mõjutab enam kui sajas riigis rohkem kui ühte viiendikku maailma elanikest (Tolba jt, 1992; WIT, 2009). Kõrbestumine põhjustab igal aastal maailmas 42,3 miljardi USA dollari ulatuses kahju (UNEP-DCB, 1991). Allika *World Atlas of Desertification* (2018) andmetel on enam kui 75% maailmas praegu kasutatavast maast degradeerunud ja 2050. aastaks võib tõenäoliselt olla viljakust kaotanud üle 90% maast, Aasia ning Aafrika on seejuures kaks sellest probleemist kõige enam mõjutatud piirkonda. Hiina on üks maailma riikidest, millele kõrbestumine on avaldanud kõige rängemat mõju (Ren jt, 2015; Shen, 2017). Hiina keskvalitsus on ammu pööranud ökoloogilisele ja keskkonnakaitsele suurt tähelepanu, see toetab piirkondlike omavalitsuste pühendumist keskkonnakaitsetegevusele kohalikul tasandil. Yulini linn üksi on alates 2012. aastast eraldanud metsanduse ökosüsteemsele tehnoloogiale ja linna haljastamisele aastas peaaegu 60,9 miljonit dollarit (CTAXNEWS, 2020). Seepärast valiti käesoleva uurimistöö objektiks Maowusu kõrb ning uurimise eesmärk oli kontrollida kaugseire kujutiste töötlemise ja analüüsimise teel uuritava piirkonna haljastamisel tehtud edusamme ning seal toimunud ökoloogilisi muutusi.

Uurimistöös püstitati kolm peamist eesmärki ning järgmised nendega seotud küsimused.

- Maowusu kõrbe taimkatte olukorra pikaajaline tuvastamine ja hindamine

K: Kuidas on Maowusu kõrbe kasvuindeks ja taimedega kaetus muutunud perioodil 1986–2020?

- Topograafilise gradiendi mõju tuvastamine Maowusu kõrbe taimedega kaetusele

K: Kas muutused taimedega kaetuses on seotud topograafilise gradiendiga?

Kuidas on taimedega kaetus muutunud erinevate topograafilise gradiendi määrade tõttu?

- Maowusu kõrbe ökoloogiliste muutuste pikaajaline tuvastamine ja hindamine.

K: Kuidas on uurimisala RSEI indeks muutunud aastattel 1990, 2005 ja 2019?

Kas NDVI, RSEI ja kolme teise näitaja (LST, NDBSI, Wet) vahel on uuritud piirkonnas tugev korrelatiivne seos? Kuidas need muutusid NDVI väärtuste suurenemise ajal?

Uurimustöös kasutatud lähteandmed, mis saadi Google Earth Engine'ist (GEE) ja pärinevad Ameerika geoloogiateenistusest (USGS), hõlmavad viiteteist NASADEM-i andmete stseeni, Landsat SR-i kogu (1. tase) ja Landsat TOA kogu (1. tase) perioodist 1986–2020.

Peaaegu kõik andmete kogumise, eeltöötluse ja töötlemisega seotud tehnilised sammud viidi läbi kasutades GEE-s Javascripte. See hõlmas näiteks Landsati kogu importimist, pilvede maskeerimist, Landsat 7 halva kvaliteediga piltide filtreerimist, igast pikslist NDVI väärtuse ning RSEI, LST, NDSI, NDVI (RSEI arvutamiseks) ja Weti väärtustena maksimaalse väärtuse võtmist. Landsati kogus käsitleti iga kaheaastast perioodi ühe perioodina ning periood 1986–2020 jagati kaheaastaste tsüklitena kaheksateistkümneks ajaperioodiks. Klassifitseerisime uuesti NDVI andmed ja RSEI andmed (LST, NDSI NDVI ja Wet koos), viisime taimedega kaetuse andmed kokku GIS tarkvaraga töödeldud DEM kõrgusandmetega ja arvutasime pärast andmete GEE-st eksportimist MATLAB-is välja indeksite korrelatsiooni.

Tulemused tõestavad, et uuritud piirkonnas tervikuna on perioodil 1986–2020 haljastus pidevalt laienenud. 1986. aastal oli uuritud ala kõrbestumise faasis ning taimedega kaetus peamiselt vähene. 2020. aastaks oli taimedega kaetus oluliselt paranenud ning oli peamiselt keskmisel või kõrgel tasemel. Teatud määral mõjutab taimedega kaetuse arengut ka topograafiline gradient. Tugevalt reljeefsel alal kaldub taimekasv olema parem kui tasasel maastikul. Vegetatsiooniindeksi kasv kiirenes uuritud piirkonnas kiiresti ning taimedega kaetus oli seal valdavalt keskmine, 10–30-kraadisel nõlval on suur taimestikuga kaetus aga oluliselt laienenud. Ökoloogiline olukord on uuritavas piirkonnas vaadeldud perioodil märgatavalt paranenud. Võrreldes 1990. aastaga suurenes öko-indeksi väärtus veidi kõigis kolmes vahemikus 0,4-0,6, 0,6-0,8 ja 0,8-1,0. Samas, vahemikes 0-0,2 ja 0,2-0,4 vastupidiselt indeksi väärtus vähenes, vahemikus 0,2-0,4 aastal 2019. kahanes Ökoloogilise Indeksi pindala 12.43. Samal ajal taimkatte suurnemisega Wet indeksi väärtused kasvased ning LSI ja NDSI väärtused kahanesid. Kuivõrd taimkate on käesoleva uurimise seisukohalt peamine näitaja ökoloogiliseks hindamiseks, näitavad kaalutud indeksi väärtused mõningast kuid ebaolulist paranemist taimkatte ökoloogilistes tingimustes.

Summary

Master Thesis Topic: Detecting the Greening of Mu Us Sand Land by using Remote Sensing

Desertification has become the focus issue of international society that affects over one-fifth of the world population in more than 100 countries (Tolba et al., 1992; WIT, 2009). Each year, desertification accounts for US$42.3 billion in economic loss worldwide (UNEP-DCB, 1991). According to the World Atlas of Desertification (2018), more than 75% of the current world's land has been degraded, and by 2050, more than 90% of the land could probably be degraded, and Asia and Africa will be the two most affected regions. China is one of the countries most seriously affected by desertification in the world (Ren et al., 2015; Shen, 2017). For a long time, the central government of China attaches great importance to ecological and environmental protection, this leads to support on regional authorities to devote to local environmental protection enterprise. Since 2012, Yulin city alone has allocated nearly US$60.9 million in forestry ecological engineering and urban greening construction every year (CTAXNEWS, 2020). Therefore, this paper decided to select Mu Us Sand Land as the object of study, our purpose in conducting this study was to check the greening achievements and ecological changes in study area by processing and analyzing remote sensing imagery.

There are three primary objectives and relevant questions as following, that were proposed in the study:

- Detecting and evaluating vegetation status in Mu Us Sand Land for long time series,

Q: How did vegetation index and coverage change in Mu Us Sand Land from 1986 to 2020

- Finding out the effect of topographic gradient on vegetation coverage in Mu Us Sand land

Q: Is vegetation coverage changing related to topographic gradient?
How did vegetation coverage change as affected by different degrees of topographic gradient?

- Detecting and evaluating ecological changes in Mu Us Sand Land for long time series.

Q: How did RSEI-based ecological index change in study area in 1990, 2005, 2019?
Is there existing a strong correlation between NDVI, RSEI, and other three indicators (LST, NDSI, Wet) in Study Area? How did they change while the increase of NDVI values?

The primary data used for the study were being acquired from google earth engine (GEE) and released by USGS, includes 15 scenes of NASADEM data, Landsat SR collection (Tier 1) and Landsat TOA collection (Tier 1) from 1986 to 2020.

Almost all of the technical steps regarding collecting, preprocessing, and processing data that finished in GEE by using Javascripts such as importing Landsat collection,

masking cloud, filtering low quality image of Landsat 7, extracting the maximum value of each pixel as the NDVI value and median values of RSEI, LST, NDBSI, NDVI (this one is for calculating RSEI), and Wet, from Landsat collection within every two years as one time period, there were 18 time periods divided with a biennial cycle in sequence from 1986 to 2020. Furthermore, we were reclassifying NDVI data and RSEI data (LST, NDBSI NDVI, and Wet attached in the same one data as bands), overlapping vegetation coverage with the processed DEM data in GIS software and calculating index correlation in MATLAB after data had been exported from GEE.

The results prove that the study area has, on the whole, maintained steady growth in greening from 1986 to 2020. In 1986, the study area was in the desertification stage, and the vegetation coverage was mainly low. By 2020, the vegetation coverage had been greatly improved, and the vegetation coverage was mainly medium and high. Furthermore, the evolution process of vegetation coverage would be affected by the topography gradient to a certain degree. The growth of vegetation in a strong relief area tends to be better than the vegetation was growing in flat terrain. The growth rate of vegetation index increased rapidly in the study area, and its vegetation coverage was mainly medium, while the high vegetation coverage has increased significantly at the range of 10-30 degrees of slope. The study area has witnessed ecological improvement during the study period. Moreover, the increase of vegetation coverage partly results in the increase in Wet and the decrease in LST and NDBSI. NDVI is only an element of RSEI but not a decisive factor that can change RSEI, an increase in NDVI without a substantial change in quality and quantity might not significantly impact ecological change. In broad terms, as of 2019, only the areas of Yulin and Shenmu located within the Mu Us Sandy Land have seen a steady increase in vegetation along with ecological improvements, but both are at a moderate level, with vegetation cover and the ecological index falling far short of the optimal range.

ACKNOWLEDGEMENTS

I am most thankful to my supervisor Prof. Tõnu Oja for his generous support, coaching, and helpful advice during my thesis journey, giving me patience and making it possible for me to produce this work.

I would like to express my pround gratitude and indebtedness to the people who have helped me in the completion of this work for thier constant motivation, valuable suggestions and timely inspirations while I have been working on the thesis.

References:

Agnew, C., Chappell, A. (1999). Drought in the Sahel. Geojournal 48(4). 299-311.

Arraiza, M.P., Santamarta, J.C., Ioras, F., García-Rodríguez, J.L., Abrudan, I.V., Korjus, H., Borála, G. (ed.) (2014). Climate Change and Restoration of Degraded Land.

Madrid:Colegio de Ingenieros de Montes.

Ambalam, K. (2014). United Nations Convention to Combat Desertification: Issue and Challenges.

Becerril-Piña R., Mastachi-Loza C.A. (2020) Desertification: Causes and Countermeasures. In: Leal Filho W., Azul A., Brandli L., Özuyar P., Wall T. (eds) Life on Land. Encyclopedia of the UN Sustainable Development Goals. Springer, Cham.

Berry, L., Ford, R.B., (1977). Recommendations for a system to monitor critical in areas prone to desertification: a report submitted to the United States Agency for International development and Department of State under contract number Aid/Ta-C-1407 on behalf of the United States Task Force on desertification, Clark: Clark University.

Bovolo, F., Ferraioli, G., Celik, T. (2018). Analysis of Multi-temporal Remote Sensing Images.

Cao, S. (2011). Impact of China's large-scale ecological restoration program on the environment and society: achievements, problems, synthesis, and applications. Crit. Rev. Environ. Sci. Technol. 41, 317–335.

Chasek, P. S., Downie, D. L., & Brown, J. W. (2016). Global environmental politics. 7th ed. Boulder, Colo.: Westview Press. Chapter: Paradigms in Global Environmental Politics.

Cherlet, M., Hutchinson, C., Reynolds, J., Hill, J., Sommer, S., von Maltitz, G. (Eds.) (2018) World Atlas of Desertification. Introduction, 1-19.

Dekker, S.C., Rietkerk, M., Bierkens, M.F.P. (2007). Coupling microscale vegetation-soil water and macroscale vegetation-precipitation feedbacks in semiarid ecosystems[J]. Global Change Biology, 13: 671-678.

Ding, Y.L., Zheng, X.M., Zhao, K., Xin, X.P., Liu, H.J. (2016). Quantifying the Impact of $NDVI_{soil}$ Determination Methods and $NDVI_{soil}$ Variability on the Estimation of Fractional Vegetation Cover in Northeast China.

Dregne, H.E. (1986). Desertification of Arid Lands. In Physics of Desertification, ed. F.El-Baz and M.H.A. Hassan. Dordrecht, The Netherlands: Martinus, Nujhoff.

Duan, H.Ch. (2013). Remote Sensing Monitoring of Aeolian Desertification in the

Horqin Sandy Land Based on Multi-sensor Remote Sensing Data.

Feng, Q., Ma, H., Jiang, X., Wang, X., Cao, S.X. (2015). What Has Caused Desertification in China?. Sci Rep 5, 15998.

Funk, C., Peterson, P., Landsfeld, M. et al. (2015). The Climate Hazards Infrared Precipitation with Stations – A New Environmental Record for Monitoring Extremes. Sci Data 2, 150066.

Gao, Y., Huang, J., Li. S,, et al. (2012). Spatial pattern of non-stationarity and scale-dependent relationships between NDVI and climatic factors-A case study in Qinghai-Tibet Plateau, China[J]. Ecological Indicators, 20(7): 170-176.

Gao, Zh.H., LI, Z.Y., Wei, H.D., Ding, F. Ding G.D., (2006). Study on the Suitability of Vegetation Indices (VI) in Arid Area. Research Institute of Forest Resources Information Techniques, Chinese Academy of Forestry, Beijing 100091,China;2. Gansu Desert Control Research Institute, Wuwei 733000,Gansu,China;3.College of Water and Soil Conservation, Beijing Forestry University, Beijing 100083,China).

GEF & GM. (2006), Resource Mobilization and the Status of Funding of Activities Related to Land Degradation, Report prepared for the Global Environment Facility (GEF) and the Global Mechanism of the United Nations Convention to Combat Desertification (UNCCD), Washington, DC.

Grabherr G, Gottfried M, Pauli H. (1994). Climate effects on mountain plants[J]. Nature, 369: 448.

Guo, J., Wang, T., Han, B.Sh., Sun, J.X., Li, X.Q. (2008). Dynamic Process of Aeolian Desertification Land Variation in Mu Us Sandy Land and Its Surrounding Area in Recent 30 Years.

Han, X.Y. (2019). Spatial and temporal dynamics and spatial autocorrelation of desertification land in Mu Us sandy land in recent 30 years.

Hu, S.G, Zhang, Z.X., Wen, Q.K., Wang, X., Liu, B., Wang, C.Y. (2010). "Fractal characters of rocky desertification land : A case study in Pingguo County, Guangxi Province, China," 2010 18th International Conference on Geoinformatics. pp. 1-5.

Hu, Y.F., Han, Y.Q., Zhang, Y.Z. (2020). Land desertification and its influencing factors in Kazakhstan. Journal of Arid Environments. Volume 180.

Huang, Y.Ch., Sun, J.G., Yan, Ch.Zh. (2014). Remote Sensing Analysis of Vegetation Cover Changes of Mu Us Sandland.

Hou, M.T., Zhao, H.Y., Wang, Z,h, Yan, X.D. (2013). Vegetation Responses to Climate Change by Using the Satellite-Derived Normalized Difference Vegetation Index： A

Review[J].Climatic and Environmental Research,18(3): 353-364

Ichii L, Kawabata A, Yamaguchi Y. (2002). Global correlation analysis for NDVI and climatic variables and NDVI trends: 1982-1990[J]. Int. J. Remote Sens., 23: 3873-3878.

IPBES. (2018): The IPBES assessment report on land degradation and restoration. Montanarella, L., Scholes, R., and Brainich, A. (eds.). Secretariat of the Intergovernmental Science-Policy Platform on Biodiversity and Ecosystems Services, Bonn, Germany. 744 pages.

IPCC. (2018): Global Warming of 1.5°C. An IPCC Special Report on the impacts of global warming of 1.5°C above pre-industrial levels.

Jia, J. G. (2018). Land Desertification Evaluation of Xinglongzhao Forest Farm in Naiman Banner.

Julien, Y., Sobrino, J. A. (2009). The yearly land cover dynamics (YLCD) method: An analysis of global vegetation from NDVI and LST parameters[J]. Remote Sens. Environ., 113: 329-334.

Kawabata, A., Ichii, K., & Yamaguchi, Y. (2001). Global Monitoring of Interannual Changes in Vegetation Activities Using NDVI and Its Relationships to Temperature and Precipitation. International Journal of Remote Sensing, 22, 1377-1382.

Kumar, R., Das, AJ. (2014). Climate Change and its Impact on Land Degradation: Imperative Need to Focus. J Climatology and Weather Forecasting 2.

Li, B.L., Zhou, Ch.H. (2002). A Study on Monitoring Sandy Desertification in Sandy Land of West Northeast China Plain.

Li, H.X,, Huang, J.J., Liang, Y.J., Wang, H., Zhang, Y.Ch.(2020). Evaluating the quality of ecological environment in Wuhan based on remote sensing ecological index[J]. Journal of Yunnan University: Natural Sciences Edition, 2020, 42(1): 81-90.

Li, Q.F., Pan, Y,, Zhou, S.l., (2019). Study on Current Status and Dynamics of Land Prone to Desertification in China[J]. FOREST RESOURCES WANAGEMENT, 0(5): 12-17.

Li,R. (2021). Shaanxi to Treat 750,000 mu of Sandy Land. Shaanxi Provincial Forestry Bureau. http://lyj.shaanxi.gov.cn/zwxx/mtbd/202103/t20210317_2156755.html

Liu, J. (2009). Dynamic Change of Vegetation Coverage by Monitoring Remote Sensing in Mu Us SandLand.

Liu, A.X., Wang, Ch.Y., Liu, Zh.J., Niu,Zh. (2004). Application of NOAA-AVHRR to Desertification Monitoring for Western China.

Liu, J., Gao, J., Ma, S., Wang, W., Zou. C. (2015). Comprehensive evaluation of eco-

environmental sensitivity in Inner Mongolia, China. China Environ. Sci., 35 (2), pp. 591-598.

Liu, J., Yin, Sh., Zhang, G.Sh., Wang, L.H., Li, H., Siqingaowa. (2009). Dynamic Change of vegetation coverage of Mu Us Sandland over the 17 years by remote sensing monitor.

Lu, T. (2014). Research on Extraction of Desertification and Sand Source Area along Qinghai-tibet Engineering Corridor and Analysis.

Ma M.G., Wang J., Wang X.M., (2006). Advance in the inter-annual variability of vegetation and its relation to climate based on remote sensing. Journal of Remote Sensing, 10 (3): 421-431.

Masek, J. G. (2006). Landsat Ecosystem Disturbance Adaptive Processing System (LEDAPS)[J].

Mainguet, M., (2012). Desertification: Natural Background and Human Mismanagement.

Misachi, J. (2020). Which Countries Have Deserts?. In World Facts.

Myneni R B, Keeling C D, Tucker C J, et al. (1997). Increased plant growth in the northern high latitudes from 1981 to 1991[J]. Nature, 386: 698-702.

NASA JPL. (2020). NASADEM Merged DEM Global 1 arc second V001 [Data set]. NASA EOSDIS Land Processes DAAC.

NFGA. (2018). Desert Culture and Sandy Industry. National Forestry and Grassland Administration.

Oindo, B.O., Skidmore, A.K. (2002). Interannual Variability of NDVI and Species Richness in Kenya. International Journal of Remote Sensing, 23, 285-298.

Olsson, L., H. Barbosa, S. Bhadwal, A. Cowie, K. Delusca, D. Flores-Renteria, K. Hermans, E. Jobbagy, W. Kurz, D. Li, D.J. Sonwa, L. (2019) Land Degradation. In: Climate Change and Land: an IPCC special report on climate change, desertification, land degradation, sustainable land management, food security, and greenhouse gas fluxes in terrestrial ecosystems [P.R. Shukla, J. Skea, E. Calvo Buendia, V. Masson-Delmotte, H.-O. Pörtner, D. C. Roberts, P. Zhai, R. Slade, S. Connors, R. van Diemen, M. Ferrat, E. Haughey, S. Luz, S. Neogi, M. Pathak, J. Petzold, J. Portugal Pereira, P. Vyas, E. Huntley, K. Kissick, M. Belkacemi, J. Malley, (eds.)].

Otterman, J. (1977). Anthropogenic impact on the albedo of the Earth [J]. Climatic Change. 1(2): 137-155.

Philippon N, Mougin E, Jarlan L, et al. 2005. Analysis of the linkages between rainfall

and land surface conditions in the West African monsoon through CMAP, ERS-WSC, and NOAA-AVHRR data[J]. J. Geophys.

Pinty, B., Verstraete, M.M. (1992). GEMI: A non-linear index to monitor global vegetation from satellites[J]. Vegetatio, 101: 15-20.

Plit, F., Plit. J., Żakowski, W.(1995). Drylands Development and Combating Desertification. 3. Desertification and drylands development in CIS countries. A-I.

Qiu, G., Bao, Y.L., Bao, Y.H., Wu, J.B. (2015). Temporal and Spatial Variation of Vegetation Analysis Based on MOD13 in Mu Us Sandy Land from 2000 to 2015.

Reining, P., (1978). Handbook on desertification indicators: based on the Science Associations' Nairobi Seminar on Desertification [M]. American Association for the Advancement of Science.

Ren, X.B., Hu, G.Y., Dong, Z.B. (2015). The Concept and Assessment of Desertification Vulnerability.

Rocchini, D., Chiarucci, A., Loisell, S.A. (2004). Testing the Spectral Variation Hypothesis by Using Satellite Multispectral Image. Acta Oecologica, 26, 117-120.

Roy, D.P., Kovalskyy, V., Zhang, H.K., Vermote, E.F., Yan, L., Kumar, S.S., Egorov, A. (2016). Characterization of Landsat-7 to Landsat-8 reflective wavelength and normalized difference vegetation index continuity.

SFA PRC. (2015). A Bulletin of Status Quo of Desertification and Sandification in China. 5th round of national desertification and sandification monitoring. State Forestry Administration, P.R.China.

SFA PRC. (2018). 40-year assessment of the Green Great Wall. State Forestry Administration, P.R.China.

Spano, D., Cesaraccio, C., Duce, P., et al. (1999). Phenological stages of natural species and their use as climate indicators[J]. International Journal of Biometeorology, 42: 124-133.

Stather, E. (2006). Germany's Engagement, In: FMECD, The Role of Governance in Combating Desertification, Berlin: GTZ Haus.

Stenseth, N.C., Mysterud, A., Ottersen G, Hurrell, J.W., Chan, K.S., Lima, M. (2002). Ecological effects of climate fluctuations[J]. Science, 297: 1292-1296.

Tucker, C.J., Fung, I.Y., Keeling, C.D., Gammon, R.H. (1986). Relationship between atmospheric CO2 variations and a satellite-derived vegetation index[J]. Nature, 319: 195-199.

Tucker, C.J., Newcomb, W.W., Los, S.O., Prince, S.D. (1991). Mean and inter-year

variation of growing-season normalized difference vegetation index for the Sahel 1981-1989 [J]. International Journal of Remote Sensing. 12(6): 1133-1135.

Tucker, C.J., Newcomb, W.W., Dregne, H.E. (1994). AVHRR data sets fir determination of desert spatial extent [J]. International Journal of Remote Sensing. 15(17):3547-3566.

Tu, Zh.F., Li, M.X., Sun, T. (2016). The Status and Trend Analysis of Desertification and Sandification.

UNCD. (1977): Desertification: An overview. In: United Nations, ed. Desertification: Its Causes and Consequences. UN Secretariat of the Conference on Desertification. 121-167.

UNEP. (1994): United Nations Convention to Combat Desertification in those countries experiencing drought and/or desertification, particularly in Africa. Text with Annexes, 71p.

UNEP. (2002): Africa Environment Outlook. Past, Present and Future Perspectives. United Nations Environmental Programme.

Walker, A.S., Robinove, C.J. (1999). Annotated bibliography of remote sensing methods for monitoring desertification [M]. U,S. Geological Survey, Circular.

Wang, K.Q., Zhao, H., Sheng, Y.W., Zhang, Sh.G., Wang, X.F., Yang, H.Y., Chao, Q. (2020). Distribution and morphological parameters of dunes in the Badain Jaran Desert based on DEM [J]. Journal of Desert Research. 40(4): 81-94.

Wang, L. C., Jiao, L., Lai, F. B., et al. (2019). Evaluation of ecological changes based on remote sensing ecological index in Manas Lake wetland, Xinjiang[J]. Acta Ecologica Sinica, 2019, 39(8): 1-9.

Wang, T. (2014) Progress in sandy desertification research of China. Journal of Geographical Sciences 14(4):387-400.

Wang. X.M. (2013). Sandy Desertification: Borne on the Wind, 58: 2395-2403.

Wells, Helen T.; Whiteley, Susan H.; Karegeannes, Carrie (1976). Origins of NASA Names (PDF). NASA History Series. Washington, D.C.: NASA. SP-4402.

WHO. (2020): Climate Change: Land Degradation and Desertification. World Health Organization.

WMO. (2005): Climate and Land Degradation. World Meteorological Organization. No.989.

Wu, W., Wang, X.Zh., Yao, F.R. (1997). Appling Remote Sensing Data For Desertification Monitoring in the Mu Us Sandy Land.

Xin, Zh.B., Xu, J.X., Zheng, W. (2008). Spatiotemporal variations of vegetation cover on the Chinese Loess Plateau (1981—2006): Impacts of climate changes and human activities[J]. Science in China (Ser. D), 51 (1): 67-78.

Xu, H.Q. (2013). A remote sensing urban ecological index and its application. Acta Ecologica Sinica, 33(24): 7853-7862.

Xu, H.Q. (2019). A new index-based built-up index (IBI) and its eco-environmental significance. Remote Sens. Technol. Appl. 2017, 3, 301-308.

Yan, F., Wu, B. (2013). Desertification progress in Mu Us Sandy Land over the past 40 years.

Yan, F., Wu, B., Wang, Y.J. (2013). Spatial and Temporal Variations of Vegetation Growth Status in Mu Us Sandy Land in 2000-2011.

Yang, J.Y., Wu, T., Pan, X.Y., Du, H.T., Li, J.L., Zhang, L., Men, X.M., Chen, Y. (2019). Ecological quality assessment of Xiongan New Area based on remote sensing ecological index.

Zhang, D.G., Liang, P., Yang, X.P., Li, H.W. (2020).The control of wind strength on the barchan to parabolic dune transition.

Zhang, Zh.P., (2006). Vegetation Pattern Changes in Mu Us Desert and the Analysis of Water Income and Expenses: a Case Study in Wu Shen County.

Zeng, N,, Yoon, J. (2009). Expansion of the world's deserts due to vegetation-albedo feedback under global warming[J]. Geophys. Res. Lett., 36, L17401

Zheng, H.J. (2019) Ecological Environment Changing Research Based on Multi-Temporal Remote Sensing Ecological Index of Guangdong-Hong Kong-Macao Greater Bay Area

Zheng, X.J., (2009). Mechanics of Wind-blown Sand Movements. Wind-Blown Sand Environment, 1-17.

Zhou, R.P. (2019). Zonation and Spatiotemporal Evolution of China’s Desertification [J]. Journal of Geo-information Science. 21(5): 675- 687.

Zhu, Z., Wang, S., Woodcock, C. E.(2015). Improvement and expansion of the Fmask algorithm: cloud, cloud shadow, and snow detection for Landsats 4–7, 8, and Sentinel 2 images[J]. Remote Sensing of Environment, 159: 269-2

Non-exclusive licence to reproduce thesis and make thesis public

I, Peng WANG

1. herewith grant the University of Tartu a free permit (non-exclusive licence) to reproduce, for the purpose of preservation, including for adding to the DSpace digital archives until the expiry of the term of copyright,

'Detecting the Greening of Mu Us Sandy Land by using Remote Sensing'

supervised by Prof. Tõnu Oja.

2. I grant the University of Tartu a permit to make the work specified in p. 1 available to the public via the web environment of the University of Tartu, including via the DSpace digital archives, under the Creative Commons licence CC BY NC ND 3.0, which allows, by giving appropriate credit to the author, to reproduce, distribute the work and communicate it to the public, and prohibits the creation of derivative works and any commercial use of the work until the expiry of the term of copyright.
3. I am aware of the fact that the author retains the rights specified in p. 1 and 2.
4. I certify that granting the non-exclusive licence does not infringe other persons' intellectual property rights or rights arising from the personal data protection legislation.

Peng WANG

TARTU, 24.05.2021